EVALUATING THE EFFECT OF DEM AND BOUNDARY CONDITION DATA FOR HYDRODYNAMIC FLOOD MODELING IN A DATA SCARCE AREA, AKAKI CATCHMENT

MSc. THESIS

BY

ABEL NEGUSSIE ALEMU

ADVISOR

ALEMSEGED TAMIRU HAILE (PhD.)

July 2021

ACEWM/AAU, ETHIOPIA

EVALUATING THE EFFECT OF DEM AND BOUNDARY CONDITION DATA FOR HYDRODYNAMIC FLOOD MODELING IN A DATA SCARCE AREA, AKAKI CATCHMENT

MSc. THESIS

BY

ABEL NEGUSSIE ALEMU

A THESIS SUBMITTED TO THE DEPARTMENT OF HYDROLOGY AND WATER RESOURCES, SCHOOL OF POSTGRADUATE STUDIES, AFRICAN CENTER OF EXCELLENCE FOR WATER MANAGEMENT (ACEWM)/ ADDISABABA UNIVERSITY (AAU) IN PARTIAL FULFILLMENT OF THE REQUIREMENTS FOR THE DEGREE OF MASTER OF SCIENCE IN WATER MANAGEMENT SPECIALIZATION (HYDROLOGY AND WATER RESOURCES).

July 2021

ACEWM/AAU, ETHIOPIA

ADVISOR THESIS SUBMISSION APPROVAL SHEET

SCHOOL OF GRADUATE STUDIES

AFRICA CENTER OF EXCELLENCY FOR WATER MANAGEMENT

ADDIS ABABA UNIVERSITY

This is to certify that the thesis entitled "**Evaluating the effect of DEM and boundary condition data for Hydrodynamic flood Modeling in a data scarce area, Akaki catchment** '' submitted in partial fulfillment of the requirements for the degree of Master's with specialization in Hydrology and Water Resources, the Graduate Program of the Water management and has been carried out by Mr. Abel Negussie Alemu under my supervision. Therefore I confirm that the student has fulfilled the requirements and hence hereby can submit the thesis to the department for defense.

_____

Dr. Alemseged Tamiru Haile

(Advisor)

_____

Date

DECLARATION

I, Abel Negussie declare that the content of this thesis is my original work with the exception of such quotations or references which have been credited to their authors or sources and this thesis has not been previously submitted to this or any other University for a degree award.

Signature……

Date……

THESIS APPROVAL PAGE

This thesis entitled "**Evaluating the effect of DEM and boundary condition data for Hydrodynamic flood modeling in a data scarce area, Akaki catchment"** is approved by Advisor, Examiners, Chairperson and Head of Africa Center of Excellence for Water Management. It is fully adequate in scope and quality, as MSc research for the degree of Master of Science in Water Management, specialization in Hydrology and Water Resources.

Dr. Alemseged Tamiru Haile	_____	_____
Advisor	Signature	Date
Dr. Dessie Nadew	_____	_____
External Examiner	Signature	Date
Dr. Getachew Tegeghe	_____	_____
Internal Examiner:	Signature	Date
Dr. Beteley Tekola	_____	_____
Chairperson:	Signature	Date
Dr. Feleke Zewge	_____	_____
Head of ACEWM	Signature	Date

ACKNOWLEDGEMENT

First and foremost, I want to thank the almighty God and His Mother, Saint Virgin Mary, for giving me strength and courage during all my works.

I would like to express my spatial gratitude to Dr. Alemseged for their support, advise, encouragement, commitment, timely response, and critical comments. Really, it is difficult to express him with words and I will not forget his contribution from the simple thing to the broad knowledge.

I would like to give my appreciation to Africa Centre of Excellence for Water Management for providing me research sponsorship and all the needed assistance.

I would like also to thank Ethiopia Geospatial Information Institute, Addis Ababa Fire and Emergency Prevention and Rescue Agency, Mr. Getahun Kebede, and the community of Akaki sub city for their help by providing the necessary data to conduct this research work.

My special heartfelt gratitude also goes to my whole family and friends for their affection and encouragement.

ABSTRACT

Accurate flood inundations mapping is challenged by data availability for model calibration and validation. In this regard, evaluating the effect of input data for improving flood inundation mapping is necessary. In this study, a high-resolution digital elevation model (DEM) of 5m × 5m was obtained from the Ethiopia Geospatial information institute. However, the high-resolution DEM (5m) was found to have some limitations in capturing the river channel geometry of Akaki. As a result, field-measured (fifteen cross-sections) data was merged with DEM to improve the accuracy of the DEM. To fill the gap of boundary condition data, water depths of a flood event were measured at upstream (for simulating the model) and middle (for evaluated simulated water levels) parts of the model domain. For the tributary river, a stage hydrograph was developed based on community consultation and channel characteristics. HEC-RAS was used in this study to perform one-dimensional (1D) flood modeling of the Akaki floodplain and HEC-GeoRAS 10.4 was used for the processing of geospatial data and analysis of water surface profile results. The limitation of the DEM to capture the channel geometry was significantly improved by using field-collected cross-sections. The type of downstream boundary condition is found significant error source in modeling the flood of Akaki. Error statistics for model simulations show that the mean absolute error of water level is 1.65m when using the uncorrected DEM as model input. However, this was reduced by half as a result of correcting the DEM. The model results show that the two tributaries have a large contribution to the flood inundation of the study area. Overall, this study demonstrates how input data source and associated errors significantly affect the accuracy of flood characteristics that are simulated by a hydrodynamic flood model. As a result, researchers and concerned institutions should develop strategies to develop data gaps for enhanced understanding of flood hazard in the Akaki catchment.

Keyword: Flood hazard, Flood inundation, Flood model, Uncertainty, HEC RAS, DEM, Akaki catchment, Addis Ababa

TABLE OF CONTENTS

ABBREVIATIONS

ASTER	Advanced Space borne Thermal Emission and Reflection Radiometer
DEM	Digital Elevation Model
FDPPA	Federal disaster prevention and preparedness Agency
FEMA	Federal Emergency Management Agency
GDP	Growth domestic product
GIE	Geospatial information Institute
GIS	Geographic information system
GLUE	Generalized likelihood uncertainty estimation
GPS	Global Positioning System
GSA	Global sensitivity analysis
HEC-RAS	Hydraulic Engineering Centre – River Analysis System
LIDAR	Light detection and ranging
NDRMC	National disaster risk management commission
NMA	National meteorological Agency
MAD	Mean absolute deviation
MSE	Mean square error
RMSE	Root mean square error
SWAT	Soil and Water assessment tool
SRTM	Shuttle Radar Topography Mission
TIN	Triangulated Irregular Network
USACE	United States Army Corps of Engineers
USGS	United States Geological Survey
USSDM	Urban spatial scenario design model

LIST OF TABLE

LIST OF FIGURE

1 INTRODUCTION

1.1 Background

Floods are known as the most destructive natural disasters in the world resulting in large damage within a short time. In Addis Ababa, flooding is the main factor that challenges the city. Rapid urbanization and population increase are major factors that cause flood damage in Addis Ababa city and lead to the reduction of green structures and increase of impervious areas (Birhanu et al., 2016). According to Abo-El-Wafa et al., (2018) increasing population density in Addis Ababa from 166 to 350 inhabitants per hectare would almost half the losses of the green infrastructure. The study by Fire & Emergency (2018) reports river overtopping and poor drainage are the major factors that cause flooding in the city. In Addis Ababa city an increase in precipitation is expected along with a possible risk of flooding (Birhanu et al., 2016). However, the spatial and temporal pattern of flooding is not well investigated for the city.

Hydrodynamic models have great potential to simulate spatial and temporal patterns of flooding. For instance, the HEC RAS model has the capability to represent the complex hydraulic conditions accurately if essential hydrological data and relatively high resolution DEM serve as model inputs (Hutanu et al., 2020). The one-dimensional (1D) component of the HEC RAS model is particularly reliable for simulating flood propagation along the main rivers (Dimitriadis et al., 2016; Lea et al., 2019). According to Nkwunonwo et al., (2020) strengths of the 1D HEC RAS model are easily flexible, simple to set up, widespread documentation, and appropriate for an extensive range of data quality. The model is computationally economical since it allows several simulations within short time.

Digital elevation model (DEM) can be obtained from different sources including satellite missions, photogrammetric methods (space borne or airborne imagery), or from traditional methods (ground survey) (Md Ali et al., 2015). According to Saksena & Merwade (2015) the LIDAR (Light Detection and Ranging) data have a better horizontal resolution (0.5m) and vertical accuracy (0.15 m-0.25 m) than the old DEM driving methods such as photogrammetry, contour survey, Radar image, cartography, and interferometry. However, the flight missions to acquire LIDAR data are expensive though it is reducing with time (Hummel et al., 2011). However, high accuracy and better resolution DEM can be generated with photogrammetric

methods using stereo aerial photos in areas of complex topography (Pulighe & Fava, 2013). Accordingly, the generated photo-based DEM has good quality and is suitable for mapping tasks. Photo-based DEMs are available and accessible to many users in the area that LIDAR data are inaccessible due to their cost.

According to Saksena & Merwade (2015), the accuracy of inundation maps is greatly affected by the quality of floodplain geometry (DEM resolution and accuracy). However, the lack of fine geometry data is a problem in many developing countries. In this case, correcting the available DEM using field data of the channel cross-section is a sound decision (Bhagabati et al., 2020). However, many studies use the DEM-based elevation data without any modification (Gebre SL, 2015). As indicated by Haile & Rientjes, (2005), this will lead to large errors in the simulated flood characteristics. Only a few researchers improved the accuracy of a river terrain using field measured elevation data for flood modeling in Ethiopia (Tarekegn et al., 2010).

The main aim of this study is to evaluate the value of flood modeling by integrating field measured cross-section data with a digital elevation model. In this study, the Hydraulic Engineering Center River Analysis System (HEC-RAS) model which can simulate steady and unsteady floods was used. HEC-GeoRAS 10.4 is the tool used for the processing of geospatial data and analysis of water surface profile results. The findings of this study are expected to attract research interest for enhancing our understanding of flood modeling in data scarce regions, like Akaki catchment which is hosting Addis Ababa city.

1.2 Problem Statement

Addis Ababa is home to 25% of the urban population and provides 50% of the Gross domestic product (GDP) growth of the country (Doyle et al., 2015). However, Flooding is the main factor that challenges the city.

On various occasions, Addis Ababa city has been affected by floods. For instance, the flood of August 1994 affected 7655 people and made 2880 people homeless (Volunteers, 1995). During 2012–2018, floods destroyed properties that worth 32,140,735 Birr and displaced 527 households (Fire & Emergency, 2018). Various scholars agree that the number of registered flood hazards, loss of resources, and the number of people affected and peak flows are increasing over time in Addis Ababa city (Birhanu et al., 2016; Jalayer et al., 2014; Fire & Emergency,

2018). Even though the Addis Ababa city Administration is investing in both structural and non-structural flood mitigation measures, these investments are not considered sufficient and are often not informed by scientific evidence.

Previously, flood vulnerability is conducted for the Addis Ababa city by (Feyissa et al., 2018; Birhanu et al., 2016; Fire & Emergency, 2018); flood mapping for little Akaki and Awash basin by Jalayer et al.,(2014); and Gebre SL, (2015) respectively. However, specifically, flood modelling is rare for the Big Akaki Rivers, where major flood hazards have happened in the past. In the previous research, the geometric data used to define the river channel and floodplain to the model was extracted from coarse DEM (30m x 30m) resolutions without any modification. Now, this study aims to fill this research gap by employing a high-resolution digital elevation model (DEM) of 5m × 5m. In addition, correction of DEM using some fifteen-field river cross-section was conducted to solve some DEM limitations in capturing the river channel geometry. Hence, the study fills a research gap in the scientific research since there is inadequate evidence of the value of integrating measured cross-section and DEM for flood modelling. Besides in the study area, the automatic water level recorder was not servicing starting from 2005. As a result, to fill the data gaps water depth measurement at upstream (for simulating the model) and downstream (for evaluated simulated water levels) locations are undertaken.

1.3 Objective and Research Questions

General Objective

The main objective of this study is to evaluate the effect of input data for hydrodynamic flood modeling in a data scarce floodplain.

The specific objectives are

- To evaluate how best the field cross-section data and DEM integrate to better represent the river channels
- To evaluate the effect of correcting the DEM derived cross-section on the simulated flood level
- To evaluate the effect of boundary conditions on the simulated flood level
- To develop flood characteristic map including flood depth, velocity, and extents

To address the above objectives, the following research questions are identified:

- Is there significant difference in simulated water level using raw and corrected DEM?
- Does upstream boundary condition (e.g. tributaries) significantly affect the pattern and magnitude of the simulated water level?
- Is there significant difference in the effect of different downstream conditions in simulated water level?
- How far does the effect of incorrect downstream boundary condition propagate in the model domain?

1.4 Scope of the study

This study mainly focuses on flood inundation mapping on Big Akaki Rivers, at Akaki sub-city. In this study, to simulate flood inundation 1D unsteady HEC RAS model was used. Here, both the river channel and flood plain was modeled as 1D. To solve some DEM (5m resolution) limitations in capturing the river channel geometry, it identified fifteen (15) locations and measurement of depth, width, and as the same time GPS are taken at each location. In this study, to improve flood inundation mapping it

was evaluated only the effect of cross-section correction and boundary condition (tributaries) on stage hydrograph. Besides, the study will attain flood inundation mapping and does not consider all aspects of the flood-like sedimentation, flood vulnerability assessment, and channel stability issues.

1.5 Significance of the study

Flood inundation mapping is very important for flood risk management. As a result, this study is essential for the policymakers and development planners to prepare an appropriate emergency action plan that minimizes the potential risks or damage that may occur because of an overflow of the river. It is also helpful to aware of the local community to protect, prevent and shift to safer places. In addition, findings of this study are expected to attract research interest for enhancing our understanding of flood modeling in data scarce regions.

2 LITERATURE REVIEW

2.1 Floods in Ethiopia

Floods are known as the most destructive natural disasters resulting in large damage within a short time. Being one of the largest countries in East Africa, Ethiopia's topography characteristics have made the country vulnerable to floods that resulted in destruction and damage to life, economy, livelihoods, infrastructure, services, and health system (FDPPA, 2007).

According to NDRMC (2018), the main cause of flooding in Ethiopia is heavy rainfall, which causes an overflow of rivers that inundates the floodplain. Flash floods are also common in some catchments of the country (OCHA, 2020). In Ethiopia, the major flood-prone areas are the Somali region along Wabe Shebelle, Genale, and Dawa Rivers; Oromia and Afar regions along Awash River (Upper, middle and lower); Amhara region along Lake Tana that surround extensive floodplain zones, Megech River, Rib River, and bank of Gumera; Gambela region along Baro, Akobo, Alwero, and Gilo Rivers; and the south nations and nationality people region along Bilate and Omo Rivers (NDRMC, 2018). Figure 2-1 shows the spatial distribution of flood-prone areas in Ethiopia.

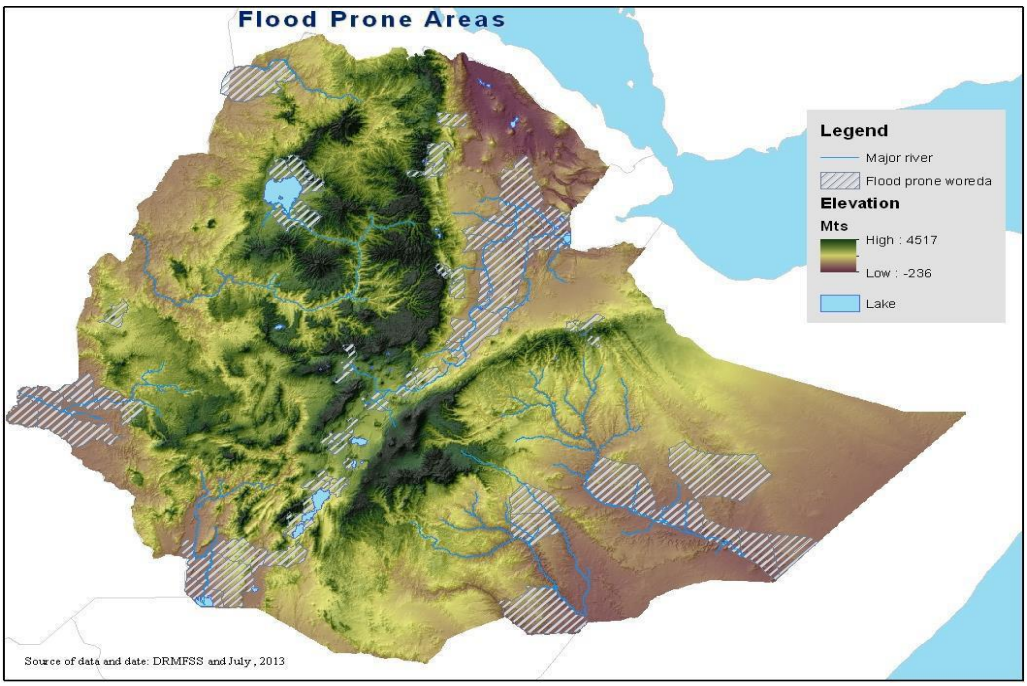

Figure 2-1 Spatial distribution of flood-prone areas in Ethiopia (NDRMC, 2018)

2.2 Flood prone areas and flood damage in Akaki and Addis Ababa

2.2.1 Flood prone areas

Addis Ababa is home to 25% of the urban population and provides 50% of the Gross domestic product (GDP) growth of the country (Doyle et al., 2015). Flooding is one of the major development challenges facing the city. The rapid economic growth and urbanization are being affected by the flood, but it is also exacerbating flooding. Urban flooding is intensified by dramatic changes in impervious areas (Douglas et al., 2008).

Various authors identified flood-prone areas in Addis Ababa city. Fire & Emergency (2018) made a study on flood vulnerability in ten sub-cities of Addis Ababa by using field surveys, questionnaires, and interviewing people. They reported that 121,000 households and 1,000 government and private institutions are vulnerable to flood disasters in the city. The study identified 143 flood hotspot areas as high risk. They stated that disasters may kill thousands and damage 4.5 billion birrs of property if the necessary relocation or reconstruction is not made soon.

The report by Fire & Emergency (2018) indicates all sub-cities of Addis Ababa have flood-prone areas. Most of the flood-prone areas are found in the Kolfe Keranio sub-city but Nifas Silk, Addis Ketema, and Akaki also have many flood-affected areas. Therefore, Addis Ababa is vulnerable to riverine as well as flash floods, and riversides in Addis Ababa have become a source of worry for residents. In the appendix, all flood-prone areas along different Rivers of Addis Ababa and their Vulnerability label are described.

Feyissa et al., (2018) applied the general exposure index to rank flood exposure in Addis Ababa. Their result showed that the following three sub-cities have the highest exposures to flooding: Addis Ketema (0.72), Arada (0.66), and Lideta (0.5). Moderate exposures were reported for Kirkos (0.45), and Gulelle (0.49). Other sub-cities have low exposure index values with the least exposure in the Bole sub-city (0.135).

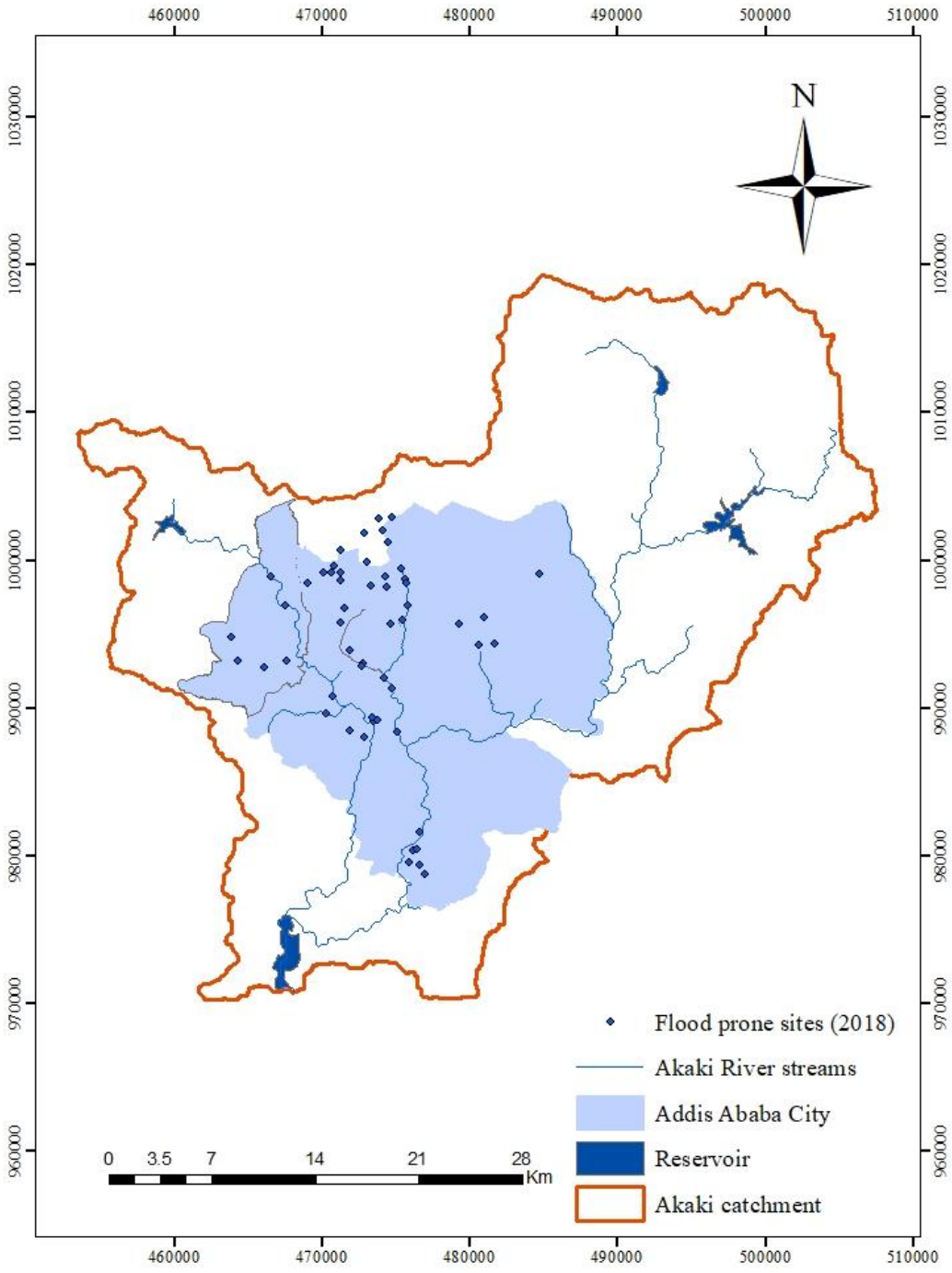

Figure 2-2 Flood-affected areas in Addis Ababa in 2018, Map was compiled and constructed by authors but Flood prone site Source: (Fire & Emergency, 2018)

Figure 2.2 shows the spatial distribution of flood-prone areas in Addis Ababa. Most of these areas are situated along the main rivers indicating overflow of these rivers is the major cause of flooding in the city. However, there are flood-prone areas that are situated far from the rivers indicated on the map. Other factors also affect flood hazards in Addis Ababa.

Flooding affects major roads of Addis Ababa during the rainy seasons (Teklie, 2017). It causes high traffic jams affecting the movement and day to day life of residents. Floods also degrade the pavement thereby creating an economic loss, and causing accidents.

As a result of increased vulnerability to flooding, the Addis Ababa, city Administration investing in both structural and non-structural flood mitigation measures (Achamyeleh, 2003). The structural intervention covers the construction of retaining walls and dikes and the improvement of river channels. The non-structural plans include reforestation and proper zoning concerning settlements close to the streams and adequate early warning. However, these investments are not considered sufficient and are often not informed by scientific evidence.

From the above review studies, various scholars agree that Addis Ababa is affected by flooding at different times. Vulnerability to riverine as well as flash floods increased and riversides have become a source of worry for residents (NMA, 2006; NDRMC, 2018).

2.2.2 Flood Damage and Risk in Akaki and Addis Ababa

On various occasions, Addis Ababa city has been affected by floods. For instance, the flood of August 1994 affected 7655 people and made 2880 people homeless (Volunteers,1995). Three people were killed and total direct flood damage has been estimated at 16.4 million Birr. This does not include indirect damages such as raising hazard vulnerability of survivors, traffic and trade disturbance, and a decrease of confidence in the area. During 2012–2018, floods destroyed properties that worth 32,140,735 Birr and displaced 527 households (Fire & Emergency, 2018).

The flood damage showed an increasing trend from 2012-2018 which might have been caused by increased flood magnitude and frequency as well as increase flood exposure by urbanization. Inadequate capacity of drainage network combined discharging waste material into the ditches (pipes) leads to increased floods along major roads. This is also supported by the findings of Birhanu et al., (2016) who applied the Soil and Water Assessment Tool (SWAT) modeling approach to show a rise in peak flow by 25% from 1993 to 2002. They calibrated the model at

the Akaki gauging station and showed that the peak flow is likely to be affected by climate change.

Table 2-1 Flood hazards and damage rates of Addis Ababa city from 2012-2018 (Fire & Emrgency, 2018)

Flood year	No. of flood hazard	Loss of resource(Birr)	People injured(No.)	Loss of life (No.)	No. of affected households
2012	8	7,778,000	2	-	24
2013	4	1,105,000	-	-	289
2014	6	943,000	-	-	12
2015	11	271,800	-	-	-
2016	15	681,035	-	-	55
2017	25	3,927,200,	-	-	-
2018	55	21,361,900	1	2	147 (only Akaki Woreda3)
Total	124	32,140,735	3	2	527

From the above review studies, various scholars agree that the number of registered flood hazards, loss of resources, and the number of people affected and peak flow are increasing over time in Addis Ababa city.

2.3 Factors Exacerbating flood damage in Addis Ababa

The major factors which lead to flood damage in Addis Ababa city are rapid urbanization and population increase, the poor drainage system, extreme climatic events, and the geographical location of the city (Doyle et al., 2015; Fire & Emergency, 2018). Rapid urbanization and population increase lead to the reduction of green structures and the increase in impervious areas. As a result, urban areas generate more surface runoff even from regular storms (Douglas et al., 2008) and the situations will be more worst when poor people settle in areas that are vulnerable to flooding such as riverine and low-lying floodplains (McGranahan et al., 2007). According to (Abo-El-Wafa et al., 2018) increasing population density in Addis Ababa from 166 to 350 inhabitants per hectare would almost half the losses of the green infrastructure.

Poor drainage is a result of drainage pipe clogging by different waste materials and sedimentation. Besides, lack of sufficient culverts and ditches in the city leads to flooding, resulting in property loss, and people may even be forced to move to escape floodwaters. According to CLUVA (2012), the poor drainage systems of Addis Ababa city intensify the risk of flooding. In addition, a decrease in river or drainage pipe depth results in a reduction of storage capacity and overflow of the river. The study by Fire & Emergency (2018) reports river overtopping and poor drainage are the major factors that cause flooding in the city. They also reported the geographical location of some places is inclined plane, sunken or trough and valley, which causes exacerbating flooding damage. The study has limitations in identifying and describing facts in-depth and they have not given detail about the flood vulnerability and cause of flooding. For instance to collect the extent of flood vulnerability, factors which lead to flood damage, and flood-prone area they used to survey and interviews but this is not enough. Therefore the data can only help as initial or starting for detailed study in the future.

In Addis Ababa city extreme climatic events lead to a rise in temperature, which exacerbates the urban heat highland effects in warm seasons, and an increase in precipitation is expected along with a possible risk of flooding. Over one century of rainfall analysis, particularly considering the rainy season (June to September) showed an increasing trend of rainfall approximately by 18 mm per decade from 1951 to 2002 (Conway et al., 2004). Also according to Birhanu et al., (2016) climate change impacts using GFDL CM2.1 indicates that the peak flow is simulated to increase by 10%.

2.4 Flood models

Model is a simplified representation of a real-world system (Borner et al., 2012). The best model is the one that gives results close to reality with the use of the least parameters and model complexity (Devia et al., 2015).

Many modeling approaches have been used in flood inundation modeling. The most common approaches include planner water surface approach, small and large cell approaches, and hydrodynamic models (i.e. one-dimensional, two-dimensional, and coupled one-dimensional and two-dimensional) (Hunter et al., 2007, Werner, 2004, Tarekegn et al.,2010).

A hydrodynamic model is mathematical models that are commonly used to simulate floods. These models solve the Saint Venant equations of continuity and momentum which is developed in 1871 (Ersoy et al., 2020). Hence, they simulate water movement by solving equations derived from applying physical laws to fluid motion with varying degrees of complexity. Nowadays there is a wide availability of numerical models with different capabilities and from different developers; some models are freely available to users while others require the purchase of a license. The widely applied models for simulation are MIKE FLOOD, HEC-RAS, LISFLOOD-FP, FLO-2D, SOBEK, TELEMAC-2D, FLDWAV, ISIS, and FLUCOMP.

1D Modeling is an economical, easy to apply, and preferred approach when the flow direction in the floodplain and the river system is predominantly along the longitudinal direction. The floodplain is represented by making use of transversal cross-sections which extend beyond both river banks and/or levees (Poretti & De Amicis, 2011). In 1D, the flow direction is only along the longitudinal direction. . The drawbacks of these models include the inability to simulate lateral diffusion of the flood wave, the discretization of topography as cross-sections rather than as a surface, and the subjectivity of cross-section location and orientation (Hutanu et al., 2020; Hunter et al., 2007).

2D HEC RAS model has the capability to represent the flood plain topography in a well manner (Costabile et al., 2020; Denn, 2014). Besides, 2D HEC RAS model has also its own limitations. For instance, during calibrating the model it require finer grids which cause the model to increase the computational times and also it requires details of information to represent a channel cross-section. Today, integrating 1D (for river flow) and 2D (for flood plain) became important to influence different existing structure like bridge, culvert in floodplains.

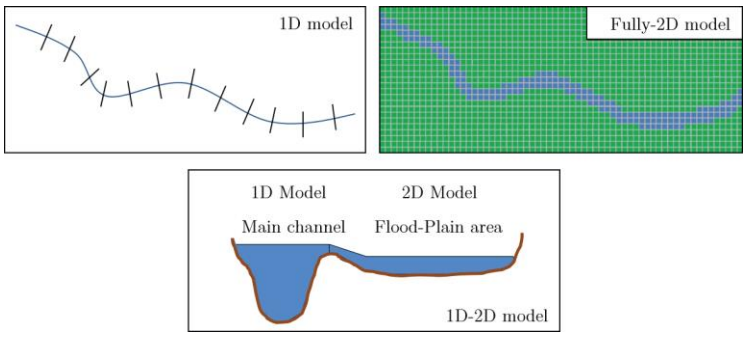

Figure 2-3 Hydrodynamic models classification(Michele et al., 2011)

One of the most popular hydrodynamic models is the HEC-RAS model which was developed by the U.S. Army Corps of Engineers (USACE). The HEC-RAS model is freely available for users (https://www.hec.usace.army.mil/).This model has a friendly graphical user interface and it was applied successfully for flood studies (Quiroga et al., 2016; Zeleňáková et al., 2019; Sahoo & Sreeja, 2017). The major reason that many researchers chose this model is due to its free availability on the internet and for its versatility to use different data sources.

Hutanu et al., (2020) a study on flood hazard and vulnerability assessment using the 1D HEC RAS model and LIDAR generated DEM data. The author conducts hazard and vulnerability assessment for recurrence intervals of 1% (100 years) and 0.1 %(1000year). The result of the model output was compared with the flood hazard map generated by the National Administration Romanian water (NARW) based on MIKESHE modeling software. Accordingly, the official NARW result and 1D HEC RAS model in terms of flood extent using recurrence interval 1% and 0.1% resulted in a difference of -25.17 km^2 and -50.69 km^2 respectively. Based on the result, the author concludes that the 1D HEC RAS model has generated a sufficiently accurate result of hazard and vulnerability assessments.

1D HEC RAS model has the capability to represent the complex hydraulic conditions accurately if essential hydrological data and good resolution DEM are provided (Hutanu et al., 2020). Besides, the 1D HEC RAS model gives good results in an area where flood propagation is along the main rivers (Dimitriadis et al., 2016; Lea et al., 2019). According to Nkwunonwo et al., (2020) strength of 1D HEC RAS model include easily flexible and simple to set up, widespread documentation, and appropriate for an extensive range of data quality. Despite the strengths, the 1D HEC RAS model has limitations of dependence on different factors such as project time and money, area characteristics, level of difficulty in the output data, and dependence on detail input data (Hutanu et al., 2020). 1D HEC RAS model has limitation or cautions in the large river basin or large-scale analysis. Because the 1D model consumes a lot of resources and time and finally underestimates the flood maps results. In addition, 1D HEC RAS model has stability problems and drawback in the area that requires multi-dimensional model approach (Nkwunonwo et al., 2020).

2.5 Flood Modeling in Akaki and Addis Ababa

Different scholars used hydrological and Hydrodynamics models to conduct their study in Addis Ababa and Akaki. For instance; Jalayer et al., (2014) mapped the flood inundation profile for various return periods (10 to 300) for the little Akaki river, which is located in the southern part of Addis. The authors used the FLO2D model (using historical rainfall records, the DEM, and the calculation of the hydrograph based on the Curve Number method) assuming a simulation time of 45 hours. In their work, only the residential areas and the main road corridors were represented well in their model. However, they ignored the green areas, industrial settings, commercial areas, and other types of land cover. The model that the author applied is commercially available and has a GIS environment for very large areal extents and involves hydraulic calculations of two-dimensional flood propagation. FLO2D has the capability to simulate urban flooding in high resolution and including the storm drain system.

Abo-El-Wafa et al., (2018) modeled the impact of population density on the green infrastructure and the implications of excluding settlement development from flood-prone areas in Addis Ababa. The author used a GIS-based urban spatial scenario design model (USSDM) whose input and output parameters are raster files. For the modeling elevation data of a 5m contour map was used. The model's structure is relatively simple. The limitation of the study is it did not consider other factors that influence urban growths transformation such as land-use zoning and major infrastructure projects. In addition defining equal weight to all factors are major limitations.

Gebre SL.(2015) mapped flood inundation areas of the Upper, Middle, and Lower Awash River Basin by using one dimensional HEC-RAS model. To compute steady flow analysis the author used a critical-based option boundary condition which is calculated from fraud number. The author uses a digital elevation model (DEM) which is downloaded from the United States Geological Survey (USGS). Limitations in the HEC-RAS steady flow simulation include the assumption that the flow is steady, the flow is gradually varied, the flow is one-dimensional, and the river channels have small slopes.

Table 2-2 Data and models used by previous studies of Akaki Catchment

Author	Study Area	Used model	Used data	Time period	DEM source and resolution
Birhanu et al., (2016)	Addis Ababa	SWAT	Weather data	1985-2004	90m SRTM
			Flow data(Akaki)	1985-2004	
			Land cover (USGS)	1993&2002	
Feyissa et al., (2018)	Addis Ababa	Sullivan and Meigh's	Weather Data (Addis Ababa, Bole and Entoto station)	1989-2016	30m (source is not mentioned)
			Soil (Ministry of water, Irrigation and Energy)	2004	
			Land cover (USGS)	2017	
			Registered flood (Fire and Emergency)	2010-1016	
			Population density	2017projected	
			Unemployment rate, literacy rate, access to tap water, access to toilet, under five mortality rate, mud (wood) house type, and activity rate	2007(CSA)	
			Road length	AARA	
Abo-El-Wafa et al., (2018)	Addis Ababa	USSDM	Slope	5m contour map	50m (from Addis Ababa Urban Planning institute)
			Land use dynamics (from EIABC)	2006-2011	
			UMT map (from EIABC)	2011	
			Projected population (from UNDESA)	2011-2025	
GebreSL.(2015)	Awash	HEC-RAS	Annual rainfall (from NMA)	1971-2007	USGS (resolution are not missioned)
			Observed daily Stream flow (from Adaitu, Hombole, Melka Kuntrie, Melka worere and Dubti stations)	1975-2008	
			Boundary condition (critical depth)		
			Soil data (from MWIE)		
			Land cover (from GLCF)		
			GCP to validate spatial extent		

2.6 Data requirements for flood inundation modeling

Flood modelling generally requires four (4) data's to simulate flood inundations (Brunner, 2016; Smith et al.,2006). This are (a) digital elevation model to represent the topography of the flood plain and channel, (b) boundary condition data (upstream, downstream and initial conditions), (c) Manning roughness value to represent the bed of the channel and flood plain (d) model validation data to evaluate the accuracy of the model.

Digital elevation model (DEM) can be obtained from different sources satellite missions, photogrammetric methods (space borne or airborne imagery), or from traditional methods (ground survey) (Md Ali et al., 2015). The SRTM (Shuttle Radar Topography Mission) filled gaps in global DEM data. Stereo viewing using digital scanner images such as ASTER (Advanced Space borne Thermal Emission and Reflection Radiometer) allows the generation of DEM data (Fujisada et al., 2020). Topographic information which has high and accurate resolution can be obtained from the LIDAR (Light Detection and Ranging). However, the flight missions to acquire LIDAR data are expensive though it is reducing with time(Hummel et al., 2011). DEMs can also be developed from traditional ground surveying (e.g. topographic contour maps) by interpolating several elevation points and economical only for a small area like Geo-archaeology (Szypula, 2019).

DEMs can be produced using stereo-photogrammetry by overlapping pairs of photograph (Cukrov, 2013). It is the conversion or reconstruction of 2D plane photograph to 3D object forms. When photographs are overlapped, 60% of photograph must be in a flight direction and 20-30% of photograph is overlain perpendicular to this. Then they digitize using photogrammetric scanner. Pulighe & Fava (2013) investigate the quality of DEM created with photogrammetric methods using stereo aerial photos in areas of complex topography. Accordingly, the generated photo based DEM has good quality and are suitable for mapping tasks. The study showed that, photo-based DEMs are very economical or cheap, affordable and readily accessible. Spatially, this data are recommended in the area that LIDAR data are inaccessible due to its expensiveness.

The horizontal and vertical accuracy of the Digital elevation model (DEM) affects the accuracy of model simulations. According to Ramsbottom & Wicks., (2003) for Rural floodplain mapping, modellers require that the DEM has a vertical accuracy of about 0.5m and a spatial

resolution of at least 10m. On the other hand, the data should capture the micro-topography over large areas for modelling urban floodplains. Hence, the vertical accuracy of up to 5cm with a spatial resolution of up to 0.5m may be needed to resolve gaps between buildings (Smith et al., 2006).

Boundary condition data are other important input data in the flood inundation mappings. In HEC RAS unsteady flood simulation boundary condition data can be flow hydrograph, stage hydrograph, stage/flow hydrograph and friction slope or normal depth (Brunner, 2016). Boundary condition data are acquired from installed gauging station in the river network having spaced between 10 km to 60 km (Stephens et al., 2012). The measured data is required to be accurate to 5% for all water levels or flow rates. Some time because of extrapolation in the rating curve, the error become much more (up to 20%) and this is much common in many sites.

In addition to upstream and downstream boundary conditions, flood models require initial boundary condition data. For instance, the initial condition in HEC RAS can be initial flow and initial elevations (Brunner, 2016). Wet or flow should be specified in the1D and 2D flow areas which means that in every cross-section water surface profile must be present to keep the model run stable. There are different methods of defining the initial condition in the HEC RAS model such as; by using a first-time step of the hydrograph, leaving to define the initial value (make blank), and by using Restart file. The initial condition increases along the flow direction unless the flow is split in a different reach.

According to Brunner (2016), as a general rule initial condition can be defined by using the first time step of the hydrograph. Even if the flow in different cross-sections is varied, they need to define the minimum value from the hydrograph in the upstream parts of the river. This method is very common and easy if there is a single reach in the study. If no initial condition is provided, then HEC RAS understand that the first time step from hydrograph is the initial boundary value. The second method is by using a restart file. This method defines boundary condition value by reading from the previous result or run of the model. This method is used when the simulation time is very long and during the model became unstable at the beginning of the simulation.

According to Brunner (2016) by defining low flow for initial boundary condition simulating unsteady flow, the condition is very difficult and causes instability of the model. In addition, the simulated water surface rapidly changes, and also the water depth changed quickly when the

time and distance are small. As a result, to solve this problem stably the modeler suggested starting the simulation by using 1% of peak flow and increasing the value up to 10% according to their necessity. If the initial boundary condition became greater than 10% the computed peak value will be higher and cause instability of the model.

The third input requirement is data for validation of the simulated flood results. The model must be validated by using independent data unless it does not give confidence in the simulated results for the future events. To validate the model, there are various observation are conducted. For instance; the water level, inundation extent, flow velocity and manning roughness of the channel and flood plain. Spatially the 2D model requires spatially distributed observed data.

The last data required are estimates of bottom roughness coefficients in the channel and floodplain. The role of these coefficients is to parameterize those energy losses not represented explicitly in the model equations. In practice, they are usually estimated by calibration, which often results in them compensating for model structural and input flow errors. As a result, it can be difficult to disentangle the contribution due to friction from that attributable to compensation. The simplest method of calibration is to calibrate using two separate global coefficients, one for the channel and the other for the floodplain (Stephens et al., 2012).

There are different methods of parameterizing roughness in the literature. In the past for the determination of the bottom friction coefficient at actual sites studies follow two methods. They measure flow velocity and topographic conditions (depth and cross-sectional area) or measure topographic conditions and physical characteristics (heights, widths, etc.) of obstacles that impede flow (Medeiros et al., 2012). After conducting a survey then manning's n values are assigned to every type of land use from the standard roughness value table (Ozdemir et al., 2013). Medeiros et al., (2012) also compared the surface roughness characteristics computed based on field measurements and those assigned by the LULC method for 24 sites in Florida. Based on the result, the author indicated that parameterizing surface roughness using NLCD land cover data is the best available practice at present.

Manning roughness is one of the important factors which affect flood modeling result unless they are not estimated properly. Most studies were used Chow(1959) and Arcement et al., (1989) manning roughness value tables as a reference. And also from the literature, the manning value for the channel ranges from 0.012 to 0.15, and for flood plain, it ranges from 0.025 to 0.16.

Table 2-3 Manning's roughness values of various studies

Author	Manning value adopt in the study	Type of bed/flood plain characteristic
Ali (2016)	0.03-0.04	more stones and weeds
	0.05-0.08	Sluggish reaches, weedy, deep pools
	0.075-0.15	very weedy reaches, deep pools, or floodways with a heavy stand of timber and underbrush
Abbas et al., (2020)	0.020 to 0.035	Sediment (channel)
Parhi, (2013)	0.025 to 0.035	flood planes having short grasses and also for straight clean having no deep pools
Abily et al., (2016)	0.015	Concrete surface
Pappenberger et al., (2007)	0.025	channel
	0.015	Pavement (flood plain)
	0.033	Grassland, farmland
	0.040	Fouling (flood plain)
	0.050	Fouling (flood plain)
	0.066	Woods and buildings
Arrighi, (2019)	0.016	Asphalt (flood plain)
Yu et al., (2015)	0.01-0.05	Channel
	0.02-0.10	Flood plain
Bhola et al., (2019)	0.025– 0.110	Agriculture, short grass to medium-dense brush
Bhola et al., (2019)	0.110–0.200	forest
	0.012–0.020	transportation, firm soil to concrete
	0.040–0.080	parks to gravels in urban areas
Bertrand et al., (2015)	0.015	Concrete surface
Sarhadi et al., (2012)	0.022 to 0.045	Halilrud reach
	0.025 to 0.051	Shur reach
	0.020 to 0.032	Malanti reach
Afshari et al., (2018)	0.03	Open water
Vojtek, (2019)	0.02	Built-up area
	0.04	Backyard garden
	0.15	Forest
	0.035	Arable land
	0.035	Grassland
	0.015	Road (asphalt)
	0.035	Channel
E.Hatzigiannakis et al., (2014)	0.025 to 0.105	Channel

2.7 Uncertainty of flood modeling

A flood inundation model is important for real time forecasting as well as for inundation mappings. For variety of reason flood mapping need to be accurate either for decision making for planner or for different company like insurances. (Teng et al., 2017; Willis et al., 2019). Therefore a full understanding of the model and the uncertainty in the modeling strategy is

important. Uncertainty analysis becomes an inseparable part of the model prediction. Different steps are followed in addressing uncertainty issues. Initially, the different sources of uncertainty are identified, then quantified, and finally ranked (Teng et al., 2017).

Specifically, the sources of uncertainty by flood inundation modeler are input data uncertainty (Digital elevation model uncertainty, channel geometry, flood plain, initial and boundary condition uncertainty, flow hydrograph or water level uncertainty, etc.), parametric uncertainty (friction coefficient values, conveyance parameters), model structure uncertainty (the uncertainty associated with the numerical model) and model assessment uncertainty (data and approaches used to validate the model) (Willis et al., 2019; Teng et al., 2017; Leupi et al., 2016; Bhola et al., 2019).

Pappenberger et al., (2006) studied the parameter uncertainty with consideration of the uncertainty in rating curves, uncertainties in the upstream, downstream, and internal (bridge) boundary conditions, and uncertainties in effective roughness values, in the one-dimensional unsteady flow model HEC-RAS. The uncertainty study in their paper is based on the generalized likelihood uncertainty estimation (GLUE) method. According to the authors, an analysis of rating curve uncertainties leads to an uncertainty of the input of 18–25% at peak discharge and different implementations of bridge structures can lead to significantly different predictions of inundation extent. Their findings illustrate the importance of the uncertainty analysis in rating curves, channel roughness, and downstream boundary in flood forecasting and flood mapping.

Abily et al., (2016) applied the spatial Global Sensitivity Analysis (GSA) approach to quantify and rank uncertainty related to the high-resolution digital elevation model. The author used the FullSWOF_2D hydrodynamic model and a Monte-Carlo approach. According to the result, the uncertainty of the high resolutions model resulted in variation of up to 1m water level. Based on the result the author also reports that Global Sensitivity Analysis (GSA) has helped to reduced variability in the output.

Bellos et al., (2017) quantified the uncertainty of roughness parameters by using a simplification of physical process and proposing of surrogate model methodology. The author used the FLOW-R2D hydrodynamic model and SWMM software to estimate effective rainfall depth. According to the resulting uncertainty of roughness coefficient is likely about 0.76m for 95%

and 0.37m for 50% confidence level. Although the methodologies have capable of simulating the flood in a fast and efficient way, the methodologies have limitations in the application of large study areas.

Bhola et al., (2019) used measured water level to reduce the uncertainty of hydrodynamic flood modeling by constraining roughness. The author used two-dimensional HEC-RAS hydrodynamic models. Accordingly, the result indicated that the uncertainty of roughness coefficient in water level is bound up to 1.26m at 90% confidence level and a minimum of 0.34m. Finally, the author suggested that a field survey is very important to reduce uncertainty in roughness parameters.

3 MATERIALS AND METHODS

3.1 Study area description

Akaki catchment which is one of the tributaries of Awash River is found in the central part of Ethiopia. The catchment hosts Addis Ababa, the capital city of Ethiopia, and other small towns, which are rapidly growing. Specifically, the study area for this study starts downstream of the confluence of Legedadi and Bulbula Rivers up to the boundary of Addis Ababa in the south direction. This part of the river is called the Big Akaki. Geographically, the study domain stretches from 8^0 50'42.2'' N to 8^0 56'24.32'' N and 38^0 44' 30.1'' E to 38^0 50'0.73'' E. The study area has a river length of 18.1 km and a lateral extent of 0.25 km to 5.3 km at both directions.

The Akaki catchment has small and main wet seasons. The main wet season is called kiremet, which starts from June to September and contributes 70% of total annual rainfall whereas the little rain is situated in Belg from mid of February to mid-April. However, the remaining months remain completely dry with no rainfall (Demlie et al.,2007). The study area has an annual average rainfall of 1005mm but varies from 771 mm to 1306 mm. The maximum rainfall amount recorded was 114.4 mm per day. This was recorded on April 8, 1989. The 25 years, 50 years, and 100 year return periods rainfall of Addis Ababa is 85.7 mm, 94.1 mm, and 102.4 mm respectively (ERA, 2013).

Previously, the Big Akaki river was measured using automatic water level measurement starting from 1981-2004 around the New bridges in downstream parts (Feyera, 2007). The River has a mean annual flow of 274.3m^3/s. The range of yearly maximum flow that was recorded from 1981 to 2004 varies from 36.5m^3/s to 693.1 m^3/s. The largest flow was recorded in August. However, the automatic recorder became out of service starting from 2005. Currently, an observer is collecting the water level twice per day although the staff gauge is repeatedly damaged by floods.

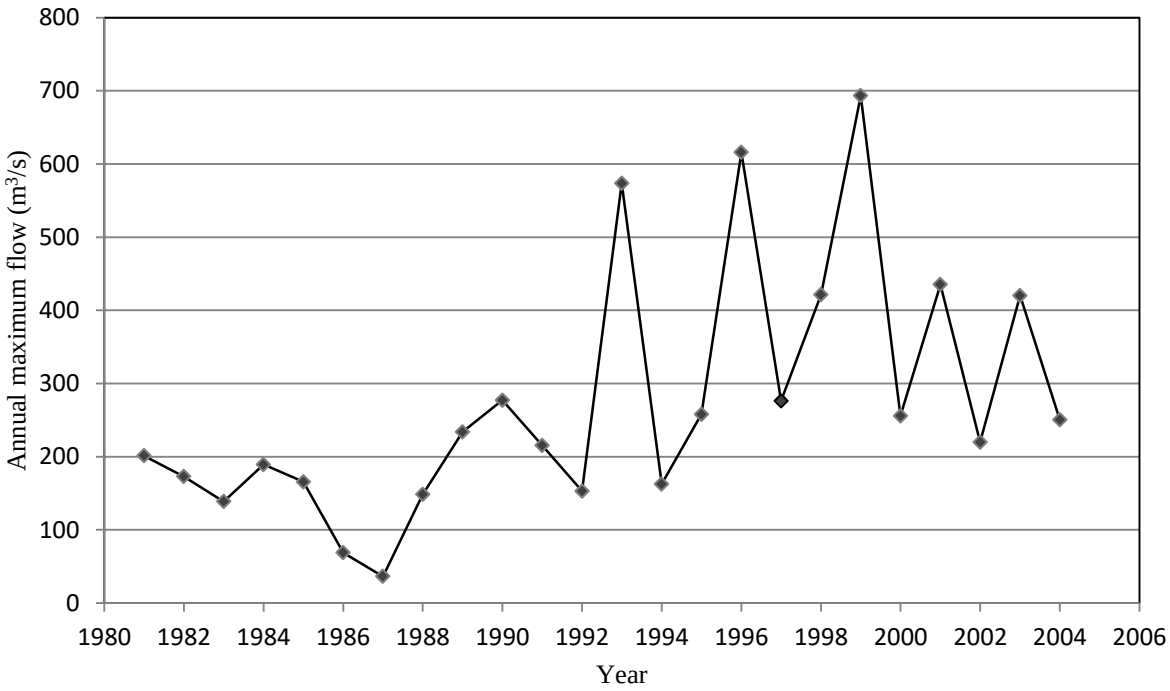

Figure 3-1 Time serious plot of annual maximum stream flow from 1981-2004

The Akaki catchment is generally categorized into four land use land cover classes: forest, urban or built-up areas, agricultural or open lands, and water body. Worako (2016) stated that land cover of the catchment at different times showed significant changes. The urban area coverage was raised from 25.71% in 1985 to 31.51% in 2015 with the expense of agricultural land reduction from 64.27% in 1985 to 56.28% in 2015.

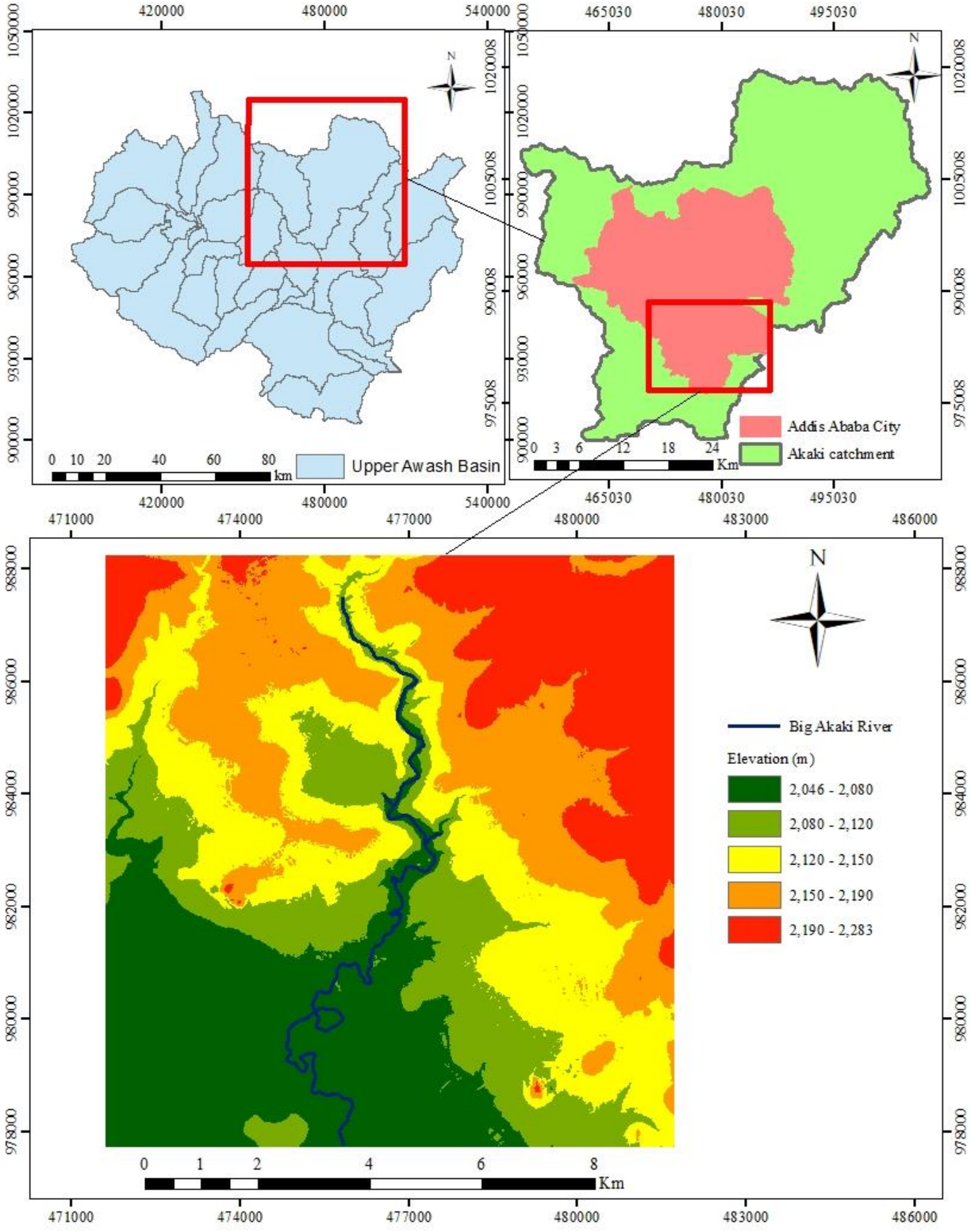

Figure 3-2 Geographic setting and elevation variation of the study area

3.2 Research Methods

3.2.1 Data sets

In this study, primary data (field data) and secondary data (from global and national archives) were collected to simulate flood extents (area), flood depth, and flood velocity. The digital elevation model (DEM) is one of the most important data for flood modeling. DEM represents the elevation of the channel and floodplain. In this study, a high-resolution digital elevation model (DEM) of 5m × 5m was obtained from the Ethiopian Geospatial Information Institute (EGII).

The field data collection consisted of cross-section surveys. This involved measurement of paired horizontal coordinates and elevation to describe the river cross-section. A measuring tape of 30 meters (100 feet) was stretched between two reference stakes. Horizontal distance was measured along with the stretched measuring tape whereas elevation was measured as depth below the measuring tape using a stick. Even if this method provides accurate measurement and was flexible in terms of selecting measurement site locations, it is time-consuming, requires at least two persons, and its accuracy is affected by the ease to access the site (i.e. deep and wide valleys and marshland is subject to errors). For this study, fifteen (15) river cross-sections were measured. The cross-section interval between two cross-sections ranged from 0.25 km to 2.2 km depending on the topographic condition and site accessibility.

Estimation of Manning's n roughness which represents a surface's resistance to flood flow in channel and floodplain requires information on land cover, channel bed conditions, and channel alignment. During the field survey, photos were taken to capture the bed material, channel alignment, and land cover. The photo that was taken from the main channel was compared against standard photos of known roughness which is usually defined based on tabulated values in hydraulics books Arcement et al., (1989). To simulate the flood, HEC-RAS requires initial, upstream, and downstream boundary condition data. In this study, stage hydrograph data was collected at upstream parts of the study area to serve as a boundary condition. In addition, water depth measurement has been conducted at the middle part of the model domain in the river to serve as a reference for evaluated simulated water levels.

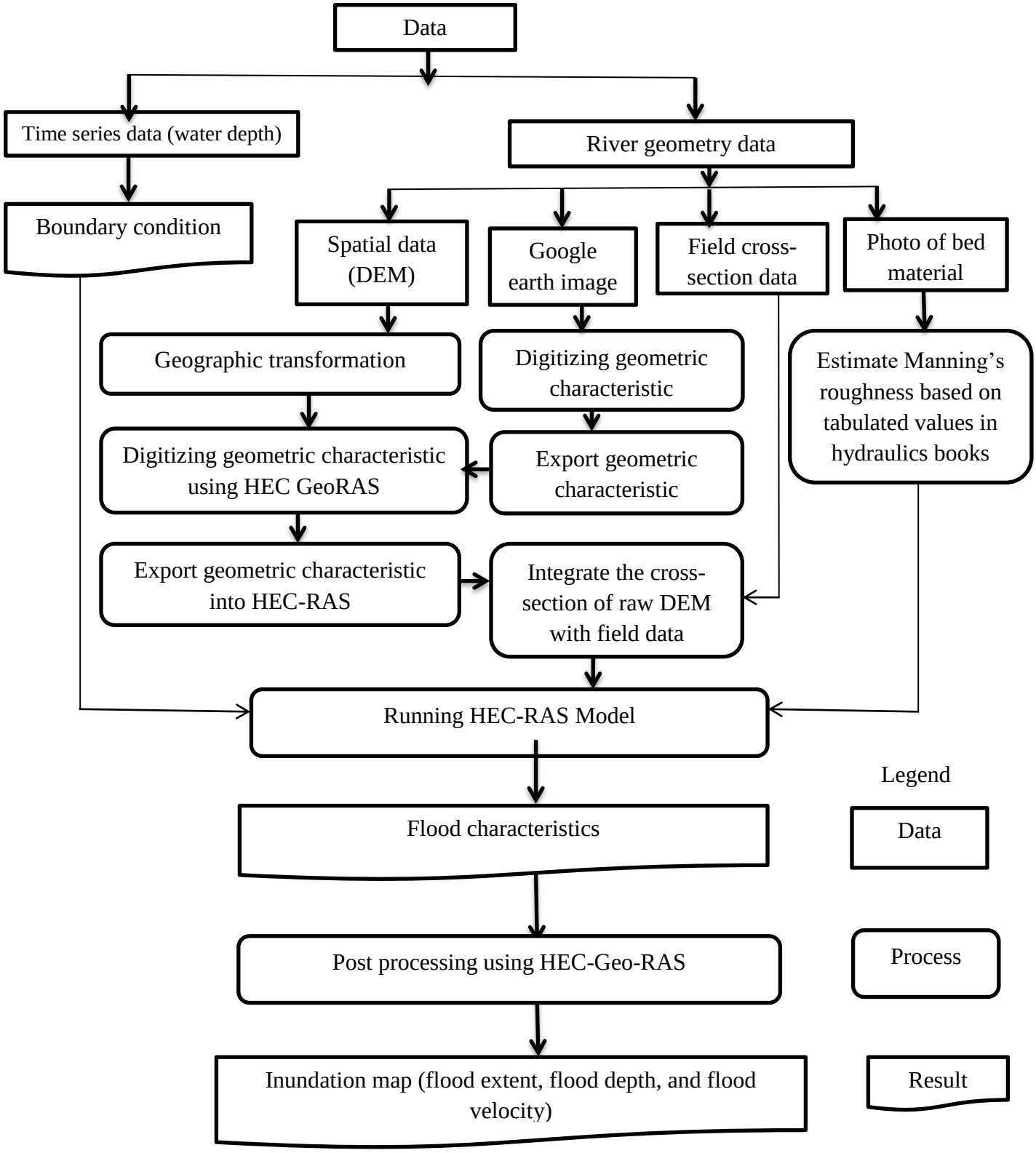

Figure 3-3 Procedure of flood Inundation Modeling

3.3 Integrating field measured cross-section data with DEM

In this study, a high-resolution Digital Elevation Model (DEM) was used, which was found to have some limitations in capturing the river channel geometry like a riverbank, channel geometry, and floodplain topography. As a result, it was found necessary to correct the DEM using field data of the channel cross-section. Accordingly, before integrating raw DEM data and field cross-section data, it was found necessary to match the geographic transformation of the DEM and field-collected cross-sections.

3.3.1 Geographic transformation

According to Hendrikse, (2003), geographic transformation is the conversion of the coordinate point of one data into another geographic coordinate by using mathematical operations. The DEM which was collected from the Geospatial Information institute (GII) was prepared using Adindan datum whereas field data was collected using WGS_1984 datum. The two datum's resulted in a distance difference of 94m and 119m along the horizontal (x) and vertical (y) directions, respectively. Hence, it was necessary to define the projection and transformation.

3.3.2 Location of field-measured cross-section data

For any hydraulic modeling, cross-section is the most important necessary input data for flood mappings. At the same time, locations of cross-section also have a very significant effect on flood modeling. If the cross-section is not properly located it might result in an error in the model outputs. From modeling approaches the more field cross-section data is the more the accuracy of the model. Here for this study, cross-sections were measured at fifteen (15) locations by measuring channel depth and width, and as the same time coordinates were recorded using hand held GPS.

Set of criteria were identified and followed to select the measurement location of cross-sections. First, the measurements were taken where there is a change in bed slope or floodplain geometry. Secondly, cross-sections were measured at bridge, culvert where there is significant obstructions of flow. Thirdly, these measurements were taken at a place where there is a change in width, depth, and roughness of the channel and floodplains. The cross-section is changed suddenly in the meandering area. Fourthly, measurement locations included locations where the banks of the river are well defined and have confined channels. Finally, even if the listed criteria are

important for measuring the cross-sections, the place must be accessible and free from an obstacle. Measuring the cross-sections in the area where there is deep and wide valleys and marshland is avoided. According to these criteria, the minimum and the maximum cross-section distance between two cross-sections are 0.25 km and 2.2 km respectively.

Figure 3-4 Sample location of field-measured cross-section data

In this study, to measure cross-section the procedures that were followed are listed below. First, stakes were installed at the lateral ends of each cross-section. Then, a rope was stretched horizontally between two reference stakes. Here, an accurate survey was required to establish the difference in elevation between the two end stakes. In this case, a sprit level was used for this purpose.

The next step was measuring the depth of the river at a different cross-section. Here, to solve the variation in channel depth across the cross-section profile, it needs to take representative measurements. This might be depending on the variability of the channel depth and the width of the river channel. Accordingly, the horizontal distance was measured along with the stretched measuring tape at 2m intervals whereas elevation was measured as depth below the measuring using a stick. Finally, site location recording was conducted. The location of the cross-section sites was recorded using a GPS.

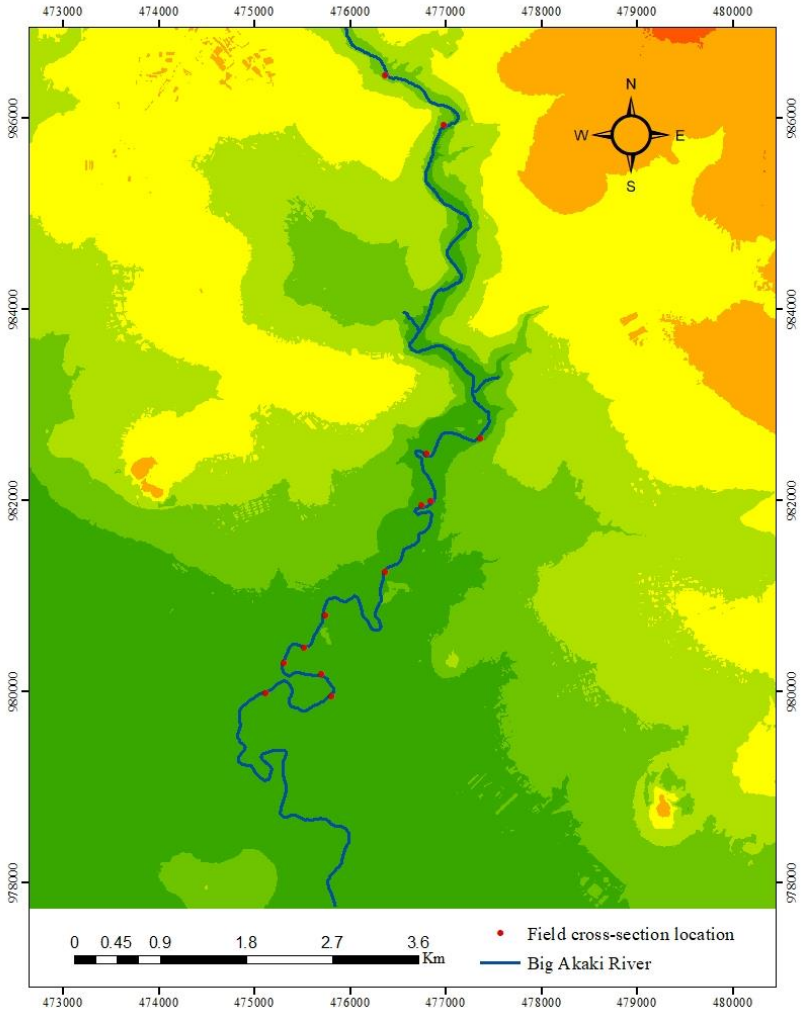

Figure 3-5 Location of field-measured cross-section data

In this study, MS excel was used to integrate field measured cross-section data with digital elevation model. The integrating technique uses the shape, depth, and width of cross-section as input for matching. If the shape of field cross-section data and the DEM cross-section were the same in the left direction, the matching will start in the left direction. However, if the shape is not matching in the left direction then it is checked for the right side of the cross-section. If both sides of the field cross-section are not matching with DEM cross-section, the matching will start from the lowest point of both field and DEM cross-section data. In this study, the shape of the cross-section from the two datasets was found to match mostly at the lowest point of the river and the left side of the river cross-sections. Finally, the three cross-section plot (uncorrected, field and corrected) was compared to visualize the difference or the error.

3.4 Preprocessing the Geometric data

This study generally followed three steps namely, preprocessing the geometric data in HEC–GeoRAS 10.4 which is an arc GIS extension, then simulating flood inundation using HEC-RAS 5.0.7 Hydrodynamic model, and finally exporting the simulated flood or water surface elevation into HEC-GeoRAS for post-processing (to determine flood extents, flood depth, and flood velocity).

In this study, flood inundation mapping was conducted for different conditions depending on the change of DEM and tributary information. As a result four models were developed for each condition (for uncorrected DEM, for corrected DEM, by considering one tributary in the corrected DEM, and by considering two tributaries in the corrected DEM). The first model was developed by using the original or raw DEM without any corrections. Whereas, the corrected one was developed by integrating the original or raw DEM with the field-collected cross-section data as described in Section 3.3. In the other case, two major tributary Rivers were identified in the left and right direction of river flow in order to evaluate their effects.

3.4.1 HEC-GEORAS

HEC-GeoRAS 10.4 is the tool used for the processing of geospatial data and analysis of water surface profile results. In this study, it was used to extract information of geometric data like river centerline, banks of river, flow path of the river, and cross-section cut lines which are essential for HEC- RAS model.

In this study, the following steps were followed to preprocess the geometric data in HEC–GeoRAS. First, spatial and 3D analysis tools were activated to create geometric data. Then, manually the river center line, banks of the river, flow path, and river cross-section cut lines were digitized one by one from Google Earth, which provides high resolution images to detect these features. These digitized data were imported into Arc GIS. Next, the DEM was added to create geometry ras layers. Here, field cross-section location data (GPS data) was needed to create a cross-section cut line in Arc GIS. Then the DEM was converted to triangulated irregular networks (TIN) to create RAS layers by using the 3D analyst tool.

The attributes in RAS layers were manually digitized in ArcGIS one by one by following the digitized data from Google Earth. Digitizing the river cross-section can be used for extracting the

elevation data from the DEM to create ground profiles across the river. Here, when digitizing the cross-section cut line it starts from left to right, it is perpendicular to the flow direction and the spacing was not too short or too long to make the model stable. Accordingly, the cross-sections were interpolated in at spacing with an interval of 50m.

Next, a unique name was assigned to the digitized data. Then, stream centerline attributes (Topology and length) and cross-section line attribute (like stationery) were assigned. Here, the station number can be used to easily identify each cross-section and to know distances between two cross-sections. Finally, the extracted cross-sectional data was exported to the HEC RAS as model input to simulate flood inundations.

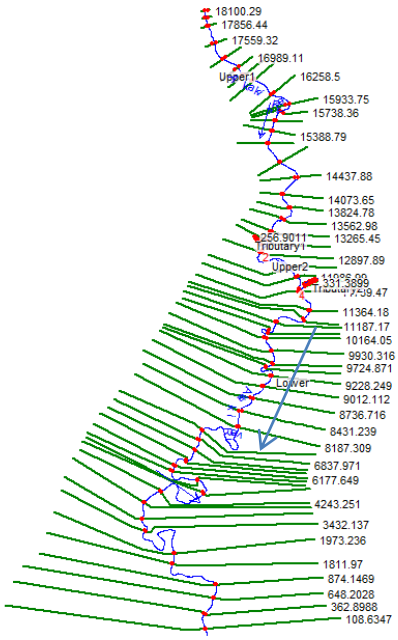

Figure 3-6 The extracted river channel profile and their cross-section cut line for 1D flood modelling using HEC-RAS

3.5 HEC-RAS model

The U.S Army Corp of Engineer's River Analysis System (HEC-RAS) was used in this study to perform one dimensional (1D) flood modelling of the Akaki floodplain. The 1D model of HEC-RAS can be used to analyze the flow in open channels (natural or artificial) and the floodplain. HEC-RAS provides data storage, ras mapper and users graphical interfaces. Many studies demonstrated that the HEC RAS model successfully simulates flood inundations (Quiroga et al., 2016, Sahoo & Sreeja, 2017). Here, both the river channel and flood plain was modeled as 1D.

3.5.1 Model Input

The main inputs of the HEC-RAS model are river geometric data (width, elevation, shape, location, and length), river floodplain data (length and elevation), distance between successive river cross-sections, Manning 'n' value for the land use type covering the river and the floodplain area, upstream and downstream boundary conditions, and initial boundary condition. The outputs from the model include water surface elevations, hydraulic properties i.e. energy grade line slope and elevation, flood extent (area), flood velocity, flood depth, and others.

In this study, a stage hydrograph was used for upstream boundary condition and normal depth or friction slope (0.01) was specified for downstream boundary conditions after sensitivity analysis. The stage data at the upstream boundary was measured for many days during the rainy season of 2020. However, it was found difficult to capture the peak flow since the peak repeatedly occurred during night which was not safe to stay at the measuring site. However, the peak was captured on 04 September 2020. Even though the hydrograph peak is captured, the measured stage did not fall to the lowest water level. As a result for this study, the hydrograph was linearly extrapolated to the water level measured on the morning of 05 September 2020. The measurement of water level (stage) was started at 9:25 AM on 04 September 2020 and lasted until 07:25 PM of the same day. As a result, the data which was measured since 04septmeber 2020 morning was used as the upstream boundary condition of the main river.

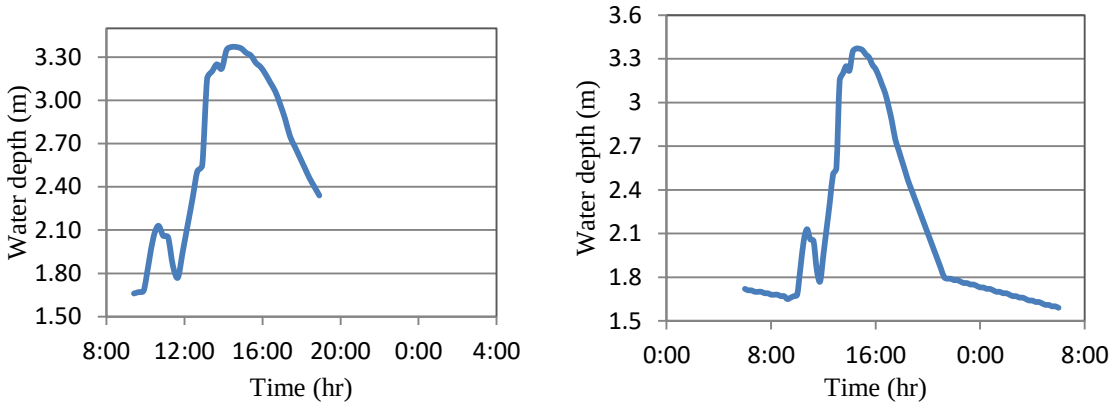

a. b.

Figure 3-7 Upstream stage hydrograph for the main river that was measured on 04 September 2020 a. before adjustment b. After adjustment

In this study, for the tributary river; measurement of boundary condition data are not taken in the field. However, the upstream boundary condition for the tributaries was identified through field visit. The channel-cross sections at the identified boundary condition sites were measured and then local people were asked to determine the maximum water level in the channel in September 2020. The peak discharge was then estimate by considering the cross-section area for the maximum water level and assuming velocity of 1m/s. Finally, the flow hydrograph was developed by adopting the shape of the stage hydrograph which was measured on the upstream boundary of the main river.

A maximum flow of 10.04 m^3/s and 39.8m^3/s were estimated for tributary 1 and tributary 2 rivers, respectively. In addition, to calculate the minimum or base flow for the tributaries, field observation of the river flow was conducted. Accordingly, for tributary 1 and tributary 2 rivers minimum flows of 1.01m^3/s and 1.04m^3/s was calculated respectively. As shown in the Figure 3-8 below the developed shapes of the flow hydrograph for the tributary are similar with the shape of the stage hydrograph of the main river with large difference in flow magnitude.

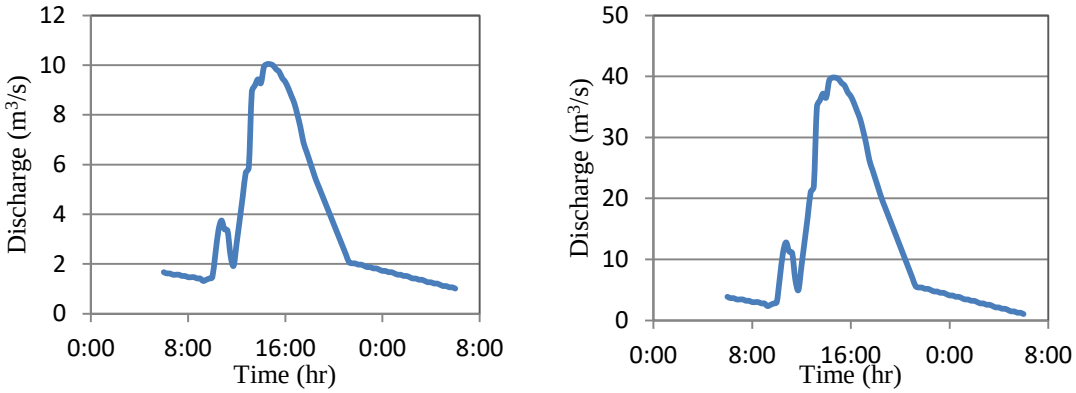

a. b.

Figure 3-8 The developed flow hydrograph for a. tributary 1 and b. tributary 2

HEC-RAS requires initialization to capture the water level prior to the actual simulation period. The model can be unstable for poorly defined initial condition data. As a result in this study, HEC RAS was run for one week before the simulation time (04 September 2020) in order to make the model more stable or to rich equilibrium. As a result, the first restart file was simulated from 28 August 2020 to 03 September 2020 using twice per day water level measurement that was obtained from Mr. Getahun Kebede, who is measuring water level in the Akaki as part of his

Ph.D. study. The simulation results were saved in a restart file which provided the initial condition for the actual simulation (i.e. 04 September 2020).

The other input data was Manning's roughness coefficients (n) which is relevant for the HEC-RAS model. Manning's roughness coefficient represents the resistance to flood flow and it is very important for accurate flood mappings. Its value depends on the channel bed and floodplain materials, irregularity (n_1), variation in channel cross section (n_2), obstructions (n_3), vegetation (n_4), and meandering (m). In this study, the information to estimate the Manning's roughness for the channel was collected from the field by visually observing and capturing a photo of the bed material (Figure 3-9) and by interviewing citizens found along the river flow lines. A Google earth satellite image was also used for the floodplain, in addition to site observation. The photo that was taken from the main channel was compared with standard photos of known roughness which is usually defined based on tabulated values in hydraulics books. In this study, the standard values in Chow(1959) and Arcement et al., (1989) were used to define Manning's roughness value. Table 3-1 shows the values of Manning's roughness coefficient used in this study.

Table 3-1 Manning's roughness value for the channel and floodplain

No.	Type of material	Manning roughness value (n)
1	gravels, cobbles, and few boulders	0.04
2	cobbles with large boulders	0.05
3	Gravel	0.035
4	Coarse sand	0.031
5	Firm soil	0.0285
6	Bare land (for flood plain)	0.025
7	Agricultural land (for flood plain)	0.033
8	Forest Land (for flood plain)	0.10
9	Urban Land (for flood plain)	0.02

a. b.

Figure 3-9 Photos of the bed material a. around upstream crusher site b. around Berta village

3.5.2 Converting field-collected water depth to water level (Elevation)

To use field-collected water depth data in the model it needs to be converted into water level (elevation) data. As a result, both collected upstream boundary condition and validation data at the middle of the model domain were converted to water level data. First, the water depth data was reported as water depth above the lowest point of the channel cross-section.

In this study, the original DEM was corrected by using field-collected cross-section data before converting the water depth data to water level. The lowest elevation on the corrected cross-sections of both upstream and middle water depth measurement locations was identified from the corrected cross-section which was extracted from DEM data. The lowest elevations of the upstream and the middle measurement sites are 2101.96 m and 2057.3 m. The measured water depth was added to these elevations to obtain the elevation of the measured water level.

3.5.3 Model accuracy and stability

In this study, several accuracy and stability problems were encounter in developing the flood model of Big Akaki. Here, in this section, the factors which make the model inaccurate and unstable along with the methods that were used to solve the problem are discussed. Cross-section spacing was the first-factor. Cross-sections must be located at a representative location to be stable and accurate. Most of the cross-section has a space distance interval between 50m to 1500m (Brunner, 2016). When the bed slope was steep and the cross-section spacing was too large, then the model became unstable and inaccurate. In a reverse, when the cross-section

spacing was too small or too close together, then the derivation with respect to distance became overestimated and it led to the model instability. In this study, the model became stable and accurate by removing cross-section which is too close together and using a spacing of 50m to interpolate and dense the cross-sections.

The selection of a preferable equation for the model was another important issue. HEC-RAS has two sets of equations to solve unsteady flow simulation. These are; the Saint Venant equation and the Diffusion Wave equation. The Diffusion Wave equation has an advantage over the Saint Venant equation to minimize computational time as it is more stable with larger computational time steps. The problem in the Diffusion Wave equation is that the change in velocity concerning time and distance is not considered. As a result, for detailed analysis and more accurate results, the Saint Venant equation is preferable (Brunner, 2016). Based on this piece of evidence the Saint Venant equation was selected for this study. Saint-Venant equation includes both conservation of mass (continuity equation) and momentum.

$$\frac{\partial A}{\partial t} + \frac{\partial Q}{\partial x} = 0 \quad \text{Continuity equation} \qquad (1)$$

$$\frac{\partial Q}{\partial t} + \frac{\partial (\frac{Q2}{A})}{\partial x} + \text{gA}\,(\frac{\partial h}{\partial x} + sf - sb) = 0 \quad \text{Momentum equation} \qquad (2)$$

Where: A = flow area (m^2); t = time (s); Q = discharge (m^3s-1); x = distance (m); g = gravitational acceleration (ms^{-2}); h = water level (with respect to the reference level in m); sf = water surface slope (m/m), sb = river bed slope (m/m).

A computational setting i.e. computational interval, mapping output interval, hydrograph output interval, and detail output interval are other problems. Computational interval is one of the most important factors which make the model inaccurate and unstable. The computational interval depends on different factors like a general rule of thumb and a courant number (Brunner, 2016). Accordingly, the selection of an appropriate time step that works in a good manner is a function of achieving results of good accuracy while minimizing the overall computation time. Generally, the recommended computational time step ranges from 1 second to 60 seconds (Brunner, 2016). In this study, a computational time step was fixed to 10 seconds after some iteration.

The H Tab parameter errors are other errors. Sometimes, the model might encounter an H Tab parameter error after all the relevant information is provided and when it was tried to run. H Tab

parameter error happened when the starting elevation of the cross-section was lower than the minimum channel elevations. This problem was solved by using the H Tab parameter editor in the geometric button. Here, it needs to identify the station which encounters the problem before solving the problem. Accordingly, the problem was solved appropriately by setting the starting elevation of the cross-section equal or slightly greater than the cross-section main channel elevations.

Computation option and tolerances were the other factors which make the model inaccurate and unstable. Water surface calculation tolerances are the most important factors from this computational option and tolerances. In the HEC RAS simulation, providing a large calculation tolerance cause instability and inaccuracy problem. In reverse, the model became more stable by making small calculation tolerance but the iteration becomes more and it increases running times (Brunner, 2016). In this study, water surface calculation tolerances of 0.0001 was provided by using trial and error.

In this study, it was used mean absolute deviation (MAD), mean square error (MSE), and root mean square error (RMSE) of accuracy measure to evaluate the accuracy of the simulated water level. According to Lee et al., (2018), these accuracy measurements are appreciable since they show errors in the units or square error of the component of interest. The result of MAD, MSE, and RMSE approximate to zero indicates that the observed and simulated value are nearly equivalent and the predicted model indicates the perfect fit. In reverse, if the observed and simulated value resulted in large variation the predicted model is considered as week. Many sholars use this error measurements to evaluate the accuracy. For instance, Bessar et al., (2020) applied MAD and RMSE of aacuracy measures to analyis uncertaintiy related to input flow and manning roughness using one dimensional(1D) HEC RAS model. The equation that was applied in order to evaluate the accuracy of the result are shown below.

$$MAD = \frac{1}{n}\sum_{i=1}^{n} abs(WLi\ sim - WLi\ obs) \quad (3)$$

$$MSE = \frac{1}{n}\sum_{i=1}^{n}(WLi\ sim - WLi\ obs)^2 \quad (4)$$

$$RMSE = \sqrt{1/n\sum_{i=1}^{n}(WLi\ sim - WLi\ obs)^2} \quad (5)$$

Where $WLi\ sim$ is the simulated water level, $WLi\ obs$ is field observed water level and n is overall number of observation presented in the given measures.

3.6 Post-processing of map layer

In post-processing, HEC-GeoRAS extracts water surface data from HEC-RAS and integrates it with a floodplain map in GIS. Water surface extent and depth was shown when floodplain maps overlaid on topographic maps. The impact associated with the extent and depth can be evaluated for the assessment of the affected features in the floodplain.

HEC-RAS computes water surface elevation for each cross-section cut line. When the water surface elevation is subtracted from terrain or digital elevation model data, the negative values indicate a flood in the area. In reverse, when water surface elevation is subtracted from terrain or digital elevation model data, positive values indicate no flood in the areas.

4 RESULTS AND DISCUSSION

4.1 Integrating field measured cross-section data with DEM

In this study, the high-resolution DEM (5m) was found to have some limitation in capturing the river channel geometry of Akaki. It was therefore found necessary to correct the DEM using field data of the channel cross-section. Figure 4-1 shows the measured cross-section at downstream location of study area around the new highway from Addis Ababa to Adama. The top width of the cross-section that was extracted from the DEM has slightly larger top width and smaller bottom width than those of the cross-section extracted from field data. It also slightly underestimated the depth to the channel bed.

This mismatch between the two cross-sections is caused by the resolution of the DEM which aggregates elevation over 5 m grid element, and the difference in data collection time of the raw DEM and field cross-section data. The DEM was generated in 2017 whereas the field data was collected in 2019. The Akaki River is undergoing rapid changes due to sedimentation and erosions as well by human interference. Figure 4-1 shows that the correction was successful in modifying the DEM cross-section to have similar characteristics as the field collected cross-section.

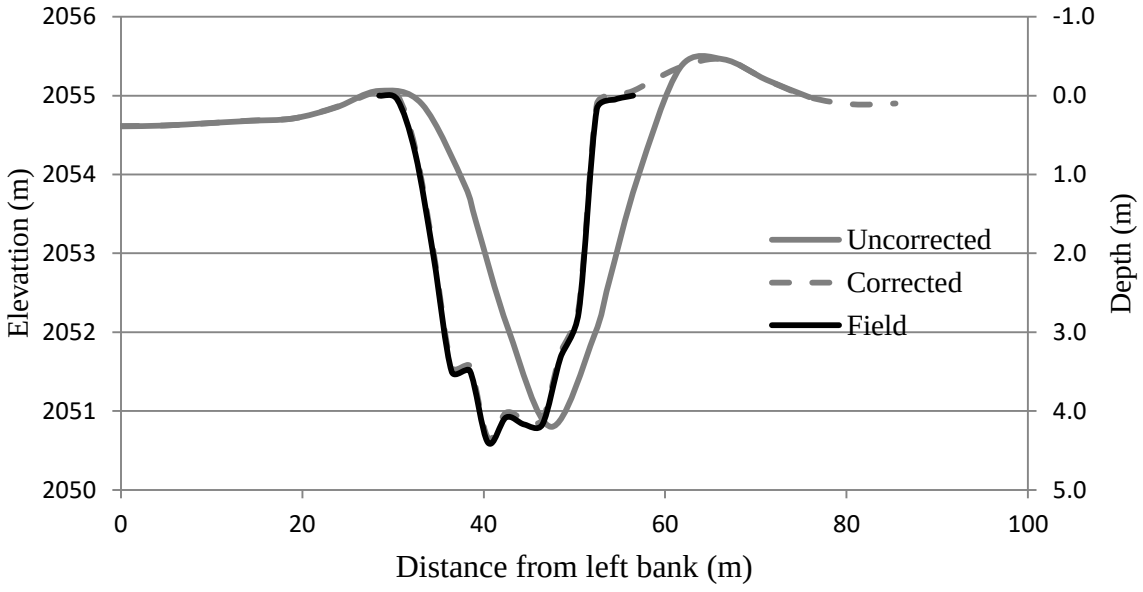

Figure 4-1 Uncorrected, Field and Corrected River cross-section profile from DEM, field data and a combination of the two (corrected) at downstream segments (around new Highway)

Figure 4-2 shows the measured cross-section at upstream location of the study area downstream the confluence of Bulbula and Legedadi rivers. The top width of the cross-section that was extracted from the DEM has slightly larger top width (in the west direction) than those of the cross-section extracted from field measured cross-section. It reasonably captured the bottom width but underestimated the depth to the channel bed. Again, the mismatch between the two cross-sections is caused by the resolution of DEM which aggregates elevation over 5 m grid element and time of the raw DEM and field cross-section data. In addition, there is human interference and erosion and sedimentation that cause rapid change of cross-section. For instance, there a crusher site that may damp materials into the river and there is ongoing construction of a bridge upstream of this site that is disturbing the channel cross-section. Figure 4-2 shows that the correction was successful in modifying the DEM cross-section to have similar characteristics as the field collected cross-section.

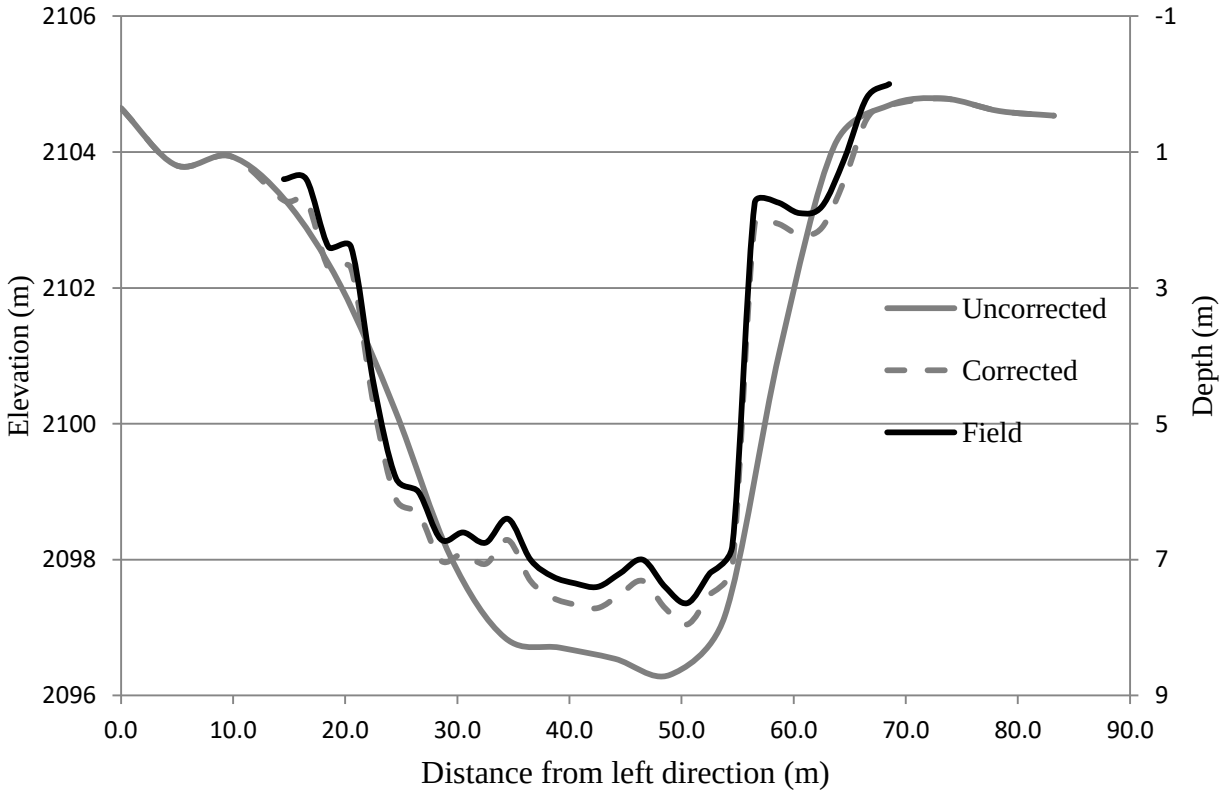

Figure 4-2 Uncorrected, Field and Corrected River cross-section profile from DEM, field data and a combination of the two (corrected) at upstream segment(around joint of Bulbula and Legedadi rives)

4.2 Sensitivity to downstream boundary condition

In this study, observed water level and discharge are missing at the downstream end of the model domain. Hence, sensitivity analysis was conducted to minimize the effect of inappropriate downstream boundary condition by locating it far away from the area of interest. Here in this research, Different downstream boundary conditions were compared, which are normal depth using friction slope, normal depth at 900m distance from the actual downstream end of the model domain, constant water level at 2052, 2053 and 2053.5 m from the downstream end. The main objective was to investigate how far the effect of uncertain boundary condition propagates upstream along the channel.

The result shows the effect of downstream boundary condition appears only near the downstream end of the river and it disappears at 3.5km upstream of the downstream boundary. Hence, the simulated flood characteristics within this distance were not used for further analysis. . Here, the constant water level causes higher water depth at the downstream end than the other boundary conditions. Whereas, specifying normal depth at 900m upstream from the downstream end causes lower water depth than that of other boundary conditions. The difference in water level caused by the remaining three downstream boundary conditions is large only up to 1500m upstream of the downstream end.

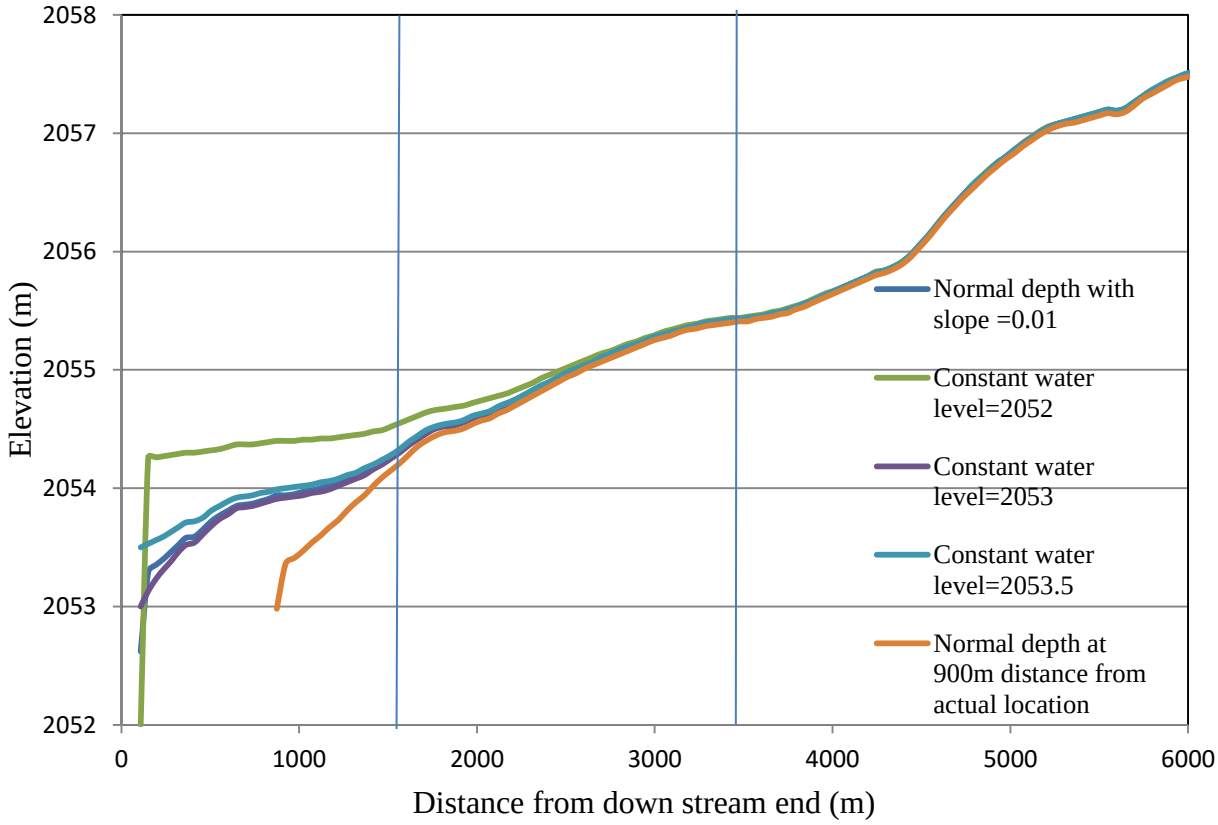

Figure 4-3 Effect of various downstream boundary conditions on the water surface elevation, that is simulated by the model.

4.3 Effect of cross-section correction on stage hydrograph

Here, the HEC-RAS model of the study domain was run using the cross-section data that was extracted from the raw DEM of 5m resolution without correction. The observed and simulated stage hydrographs are presented in Figure 4-4a for comparison. The overall pattern of the observed hydrograph is captured by the model. The slopes of the observed rising and falling limbs are well captured. However, there are two major mismatches between the two hydrographs (i) a large mismatch between the peak magnitudes, and (ii) mismatch between times to peak. The peak of the simulated stage is 2060.94 m that shows a large underestimation of the observed stage (2062.47m) by 1.53m. The time of the peak flow was simulated as 11:00 hours but the peak was observed at 8:50 hour. This implies the simulated time of the peak is delayed by 2:10 hours.

Besides, the HEC-RAS model of the study domain was run by using corrected and raw DEM of 5m resolution. For comparison, the observed and simulated stage hydrographs are presented in Figure 4-4b below. The overall pattern of the observed hydrograph is captured by the model. The slopes of the observed rising and falling limbs are well captured. Here also there is mismatch between two hydrographs in terms of peak magnitude and time to peak. The peak of the simulated stage is 2061.52 m that shows an underestimation of the observed stage (2062.47m). However, integrating field collected cross-section data with original cross-section data results in significant reduction in difference of peak magnitudes between two hydrographs from 1.53m to 0.95m. This means integrating field cross-section data with raw DEM increases the model performance. The time of the peak flow was simulated as 10:00 hours but the peak was observed at 8:50 hour. This implies the simulated time of the peak is delayed by 1:10 hours.

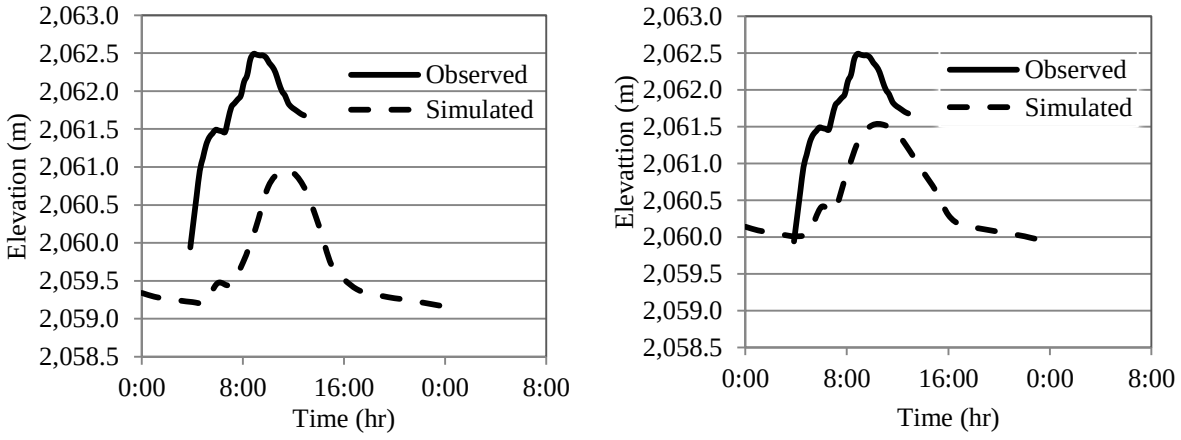

Figure 4-4 Simulated hydrograph (a) using Uncorrected DEM, (b) using corrected DEM, and observed stage hydrograph

4.4 Effect of River tributary on stage hydrograph

The HEC-RAS model of the study domain was run by considering one river tributary on the corrected cross-section DEM. For comparison, the observed and simulated stage hydrographs are presented in Figure 4-5b. The overall pattern of the observed hydrograph is captured by the model. The slopes of the observed rising and falling limbs are well captured. By considering the contribution of one tributary in the model, the peak of the simulated stage is 2062.33 m that shows a small underestimation of the observed stage (2062.47m). This means consideration of river tributary in the model simulation results in reduction of the difference in the peak river

stage between observed and simulated from 0.95m to 0.14m. The time of the peak flow was simulated as 11:00 hours but the peak was observed at 8:50 hour. This implies the simulated time of the peak is delayed by 2:10 hours.

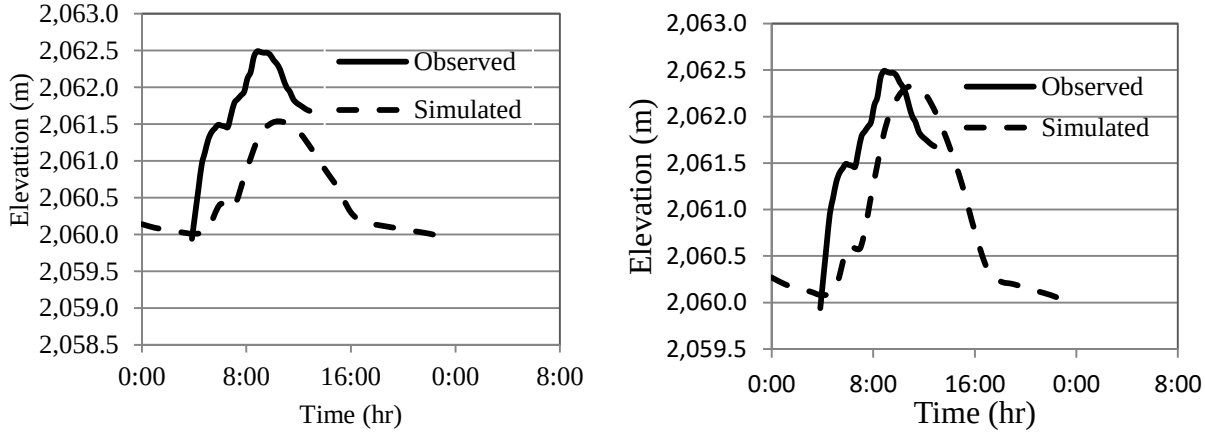

(a) (b)

Figure 4-5 Simulated and observed stage hydrograph for (a) using Corrected DEM, (b) using corrected DEM by considering one tributary

The HEC-RAS model of the study domain was also run by considering two river tributaries. Figure 4-6b shows the observed and simulated stage hydrographs. The overall pattern of the observed hydrograph is captured by the model. The slopes of the observed rising and falling limbs are well captured. By considering two tributaries in the model, the peak of the simulated stage is 2062.41 m that shows a very small underestimation of the observed stage (2062.47m). This indicates reduction of the difference between the observed and simulated peak river stages from 0.14m to 0.06m. Besides, the time of the peak flow was simulated as 11:00 hours but the peak was observed at 8:50 hour. This implies the simulated time of the peak is delayed by 2:10 hours.

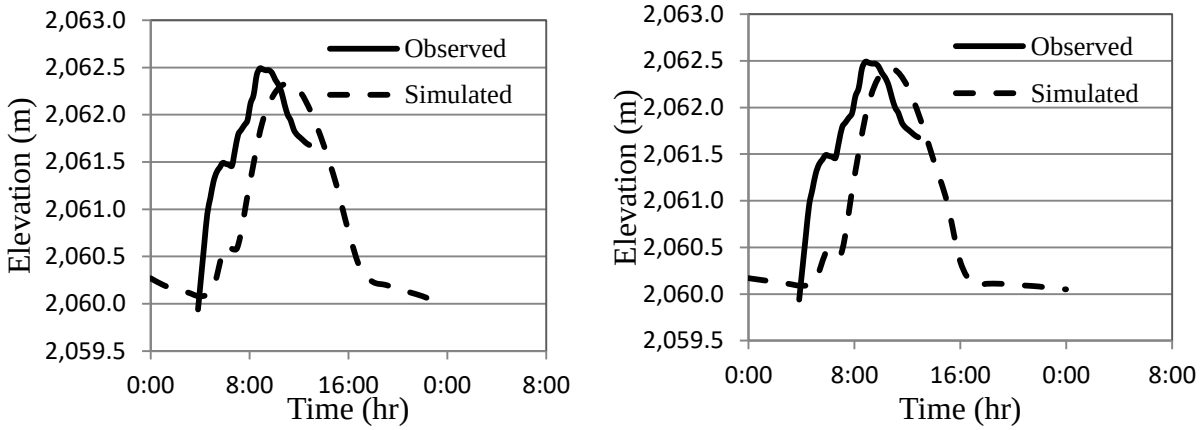

Figure 4-6 Simulated and observed stage hydrographs using (a) Corrected DEM considering one tributary, (b) corrected DEM by considering two tributaries

Table 4-1 summarizes the error statistics for model simulations using different conditions of DEM and tributary information. The mean absolute deviation was large (1.65m) when the uncorrected DEM was used and contribution of the tributaries is not considered. This significantly reduced to 0.84m when the DEM was corrected using field measured cross-section data, and dropped to 0.36m when the contribution of one tributary is considered. However, considering the second tributary slightly deteriorated the accuracy in terms of mean absolute error.

As a result, from all conditions considering only one tributary (in addition to the main river flow) has relatively small mean square error (MSE) and root mean square error (RMSE) of 0.48 and 0.69 respectively. This implies the model has good performance in capturing the observed value. Whereas, among all conditions the uncorrected DEM has very high mean square error (MSE) and root mean square error (RMSE) of 3.05 and 1.75 respectively. This implies the model has low performance in capturing the observed value.

Table 4-1 Summary of the error statistics for the simulated water level using different model inputs

Error Type (MAD,MSE & RMSE)	Uncorrected DEM	Corrected DEM	Corrected DEM by considering one tributary	Corrected DEM by considering two tributaries
Mean absolute deviation (m)	1.65	0.84	0.36	0.43
Mean square error (m^2)	3.05	0.86	0.48	0.50
Root mean square error (m)	1.75	0.93	0.69	0.71

4.5 Flood Inundation mapping

Table 4-2 shows the summary of simulated flood characteristics (flood extent, flood depth at 90^{th} percentile, and flood velocity at 90^{th} percentile) in the model domain for different DEM and tributary information. The simulation using the uncorrected DEM results in the smallest flood inundation extent whereas consideration of the two tributaries has relatively high flood extent. Overall, difference of the input data source results in up to 0.21 km^2 (=2.95-2.74) difference in the simulated flood extent.

Besides, the resulted flood depth was small (8.03m) when the uncorrected DEM was used and contribution of the tributaries is not considered. This significantly increases to 8.52 when the DEM was corrected using field measured cross-section data and further increases to 9.42m when the contribution of one tributary is considered. However, considering the second tributary slightly decrease the flood depth (by 0.17m) as compare to one tributary consideration. Overall, difference of the input data source results in up to 1.22m (=9.25-8.03) difference in the simulated flood depth.

Finally, the resulted flood velocity was small (9.49m/s) when the uncorrected DEM was used and contribution of the tributaries is not considered. This significantly increases to 10.5m/s when the DEM was corrected using field measured cross-section data and further increases to 16.12m/s when the contribution of one tributary is considered. However, considering the second tributary significantly increases the flood velocity to 24.06m/s. overall, difference of the input data source results in up to 14.57 m/s (=24.06-9.49) difference in the simulated flood velocity.

Table 4-2 Summary of flood inundation output as DEM and tributary information changes

Flood inundation out put	Uncorrected DEM	Corrected DEM	Corrected DEM by considering one tributary	Corrected DEM by considering two tributary
Flow extent (area) km^2	2.74	2.87	2.91	2.95
Flow depth (m) at 90^{th} percentile	8.03	8.52	9.42	9.25
Flood velocity (m/s) at 90^{th} percentile	9.49	10.50	16.12	24.06

Here in the figure 4-7 below describes inundation areas under each flood depth class for each condition. The effect of input data source is very distinct for flood depth less than 1.5m and that higher than 1.5m. For low flood depths, the uncorrected depth always resulted in larger flood extent, and the extent decreases as corrections are added to the DEM and tributary information. For high flood depths, the uncorrected DEM resulted in the smallest flood extent whereas the extent increased as correction or details are added to the input data. From the listed flood depth class, the forth (1.0m-1.5 m) class has relatively constitute high flooded areas in most cases. In other cases, the first flood depth class (0.0 – 0.1m) has a relatively small flooded area from all flood depth class. In addition, the flood depth class less than 2 m or from (0.0m-2.0 m) has constituted 66.7% of the total inundated area and flood depth class less than 3 m or from (0.0m-3.0 m) has constituted 81.3% of the total inundated area.

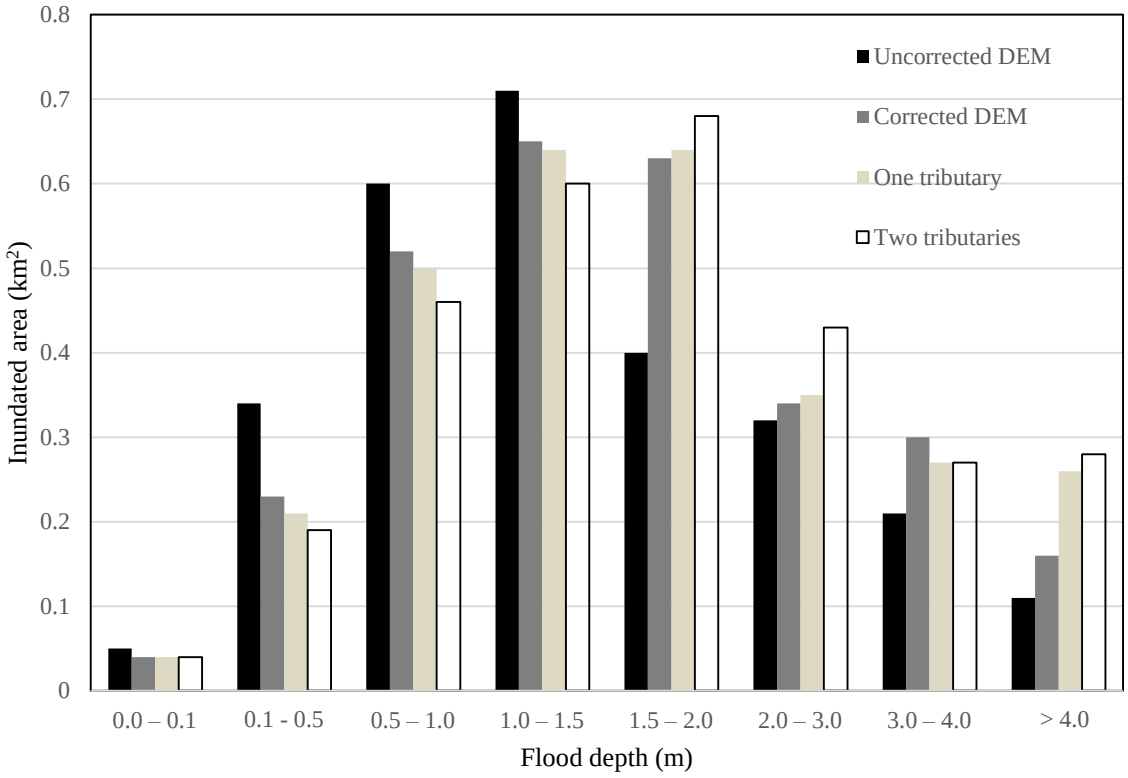

Figure 4-7 Summaries of inundated areas (km^2) under each flood depth class

Here also in the figure 4-8 below describes inundation areas under each flood velocity class for each condition. The effect of input data source is slightly great for flood velocity greater than 0.2m/s. For both high flood velocity, the uncorrected depth resulted in smallest flood extent, and in most cases the extent remain smallest as corrections are added to the DEM and tributary information. Consideration of two tributary at high flood velocity, resulted highest inundation extents and it became smallest at low flood velocity. The third velocity class (0.5-1.0) has relatively equal inundation area for all conditions except consideration of one tributary. From the listed flood velocity class, the last (>1.5 m/s) class has relatively constitute high flooded areas from all conditions. In other cases, the first flood velocity class (0.0- 0.2 m/s) has a relatively small flooded area from all conditions. In addition, flood velocity class less than 1.0 m/s or from (0.0-1.0m/s) constitute approximately 48% of the total flood area and whereas flood velocity class less than 1.5m/s or from (0.0-1.5m/s) constitute approximately 66% of the total flood area.

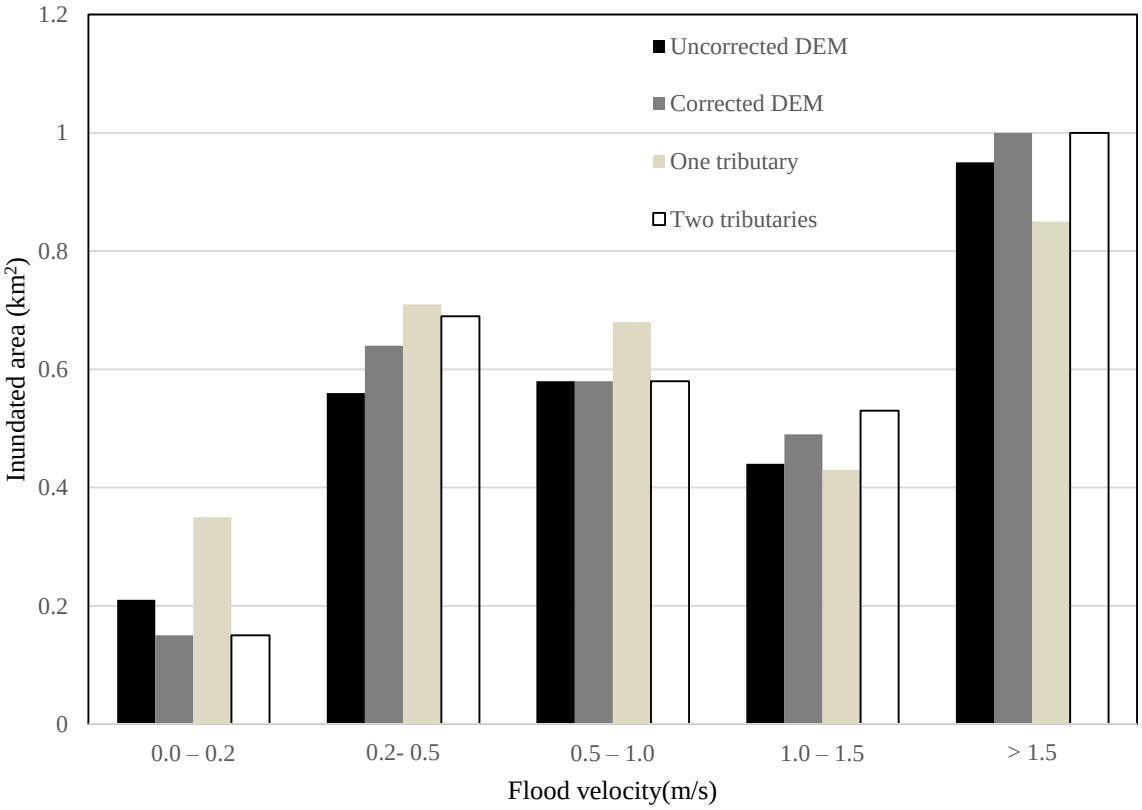

Figure 4-8 Summaries of inundated areas under each flood velocity class

Figure 1-9 shows the maximum flood depth map for the HEC-RAS model of the study domain that was run by considering two river tributaries and cross-sections from the corrected DEM. The study area has a 90^{th} percentile flood depth and flood extent (area affected by flood) of 9.25 m and 2.95km^2 respectively. The flood has high depth near the river channel and when it overflows upstream of the Akaki bridge. There is a very distinct difference between the flood depth and pattern upstream and downstream of the Akaki Bridge. The area downstream of the Akaki Bridge has relatively widespread flood extent which has relatively small depth as compared to the upstream area. However, the flood depth is large enough to cause serious damage to people and property. The flood extends out of the channel bank up to 1 km to the left side facing downstream of floodplain and it extends up to 0.5 km to the right side facing downstream of floodplain along flow direction.

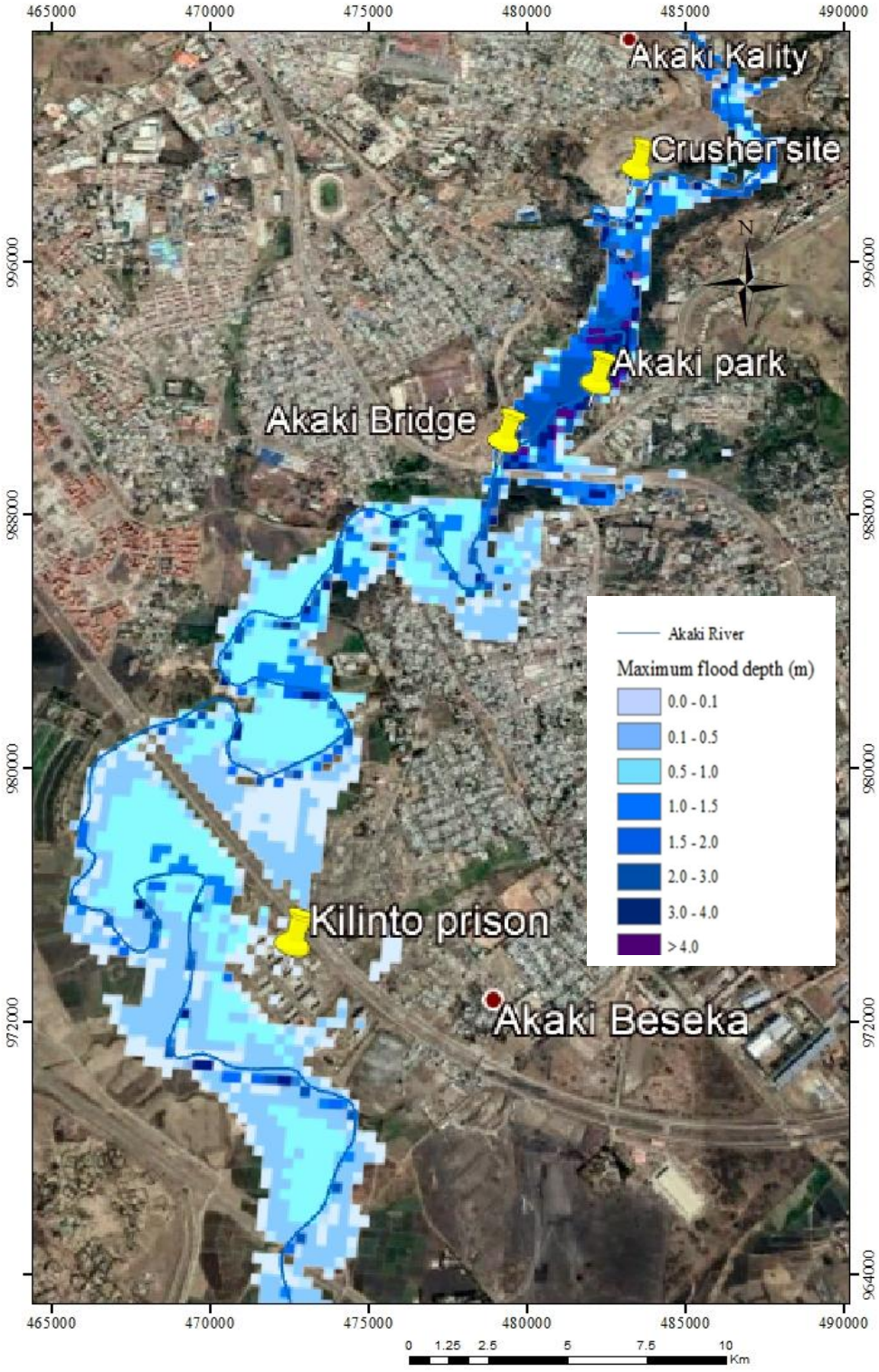

Figure 4-9 Maximum flood depth map for the simulation using two tributaries and channel cross-sections from the corrected DEM

In the figure 4-10 below shows the maximum flood velocity map for the HEC-RAS model of the study domain that was run by considering two river tributaries and cross-section from the corrected DEM. The study area has flood velocity of 24.06 m/s at 90th percentile. The flood has high velocity near the river channel and it reduces in the floodplain. The upstream parts of the study area around joint of Main River and the first tributary have high flood velocity. Whereas, around the Akaki new bridge having flood velocity up to 1.57m/s. The area downstream of the Akaki Bridge has relatively widespread flood extent which has relatively small velocity as compared to the upstream area. However, the flood velocity is large enough to cause serious damage to people and property.

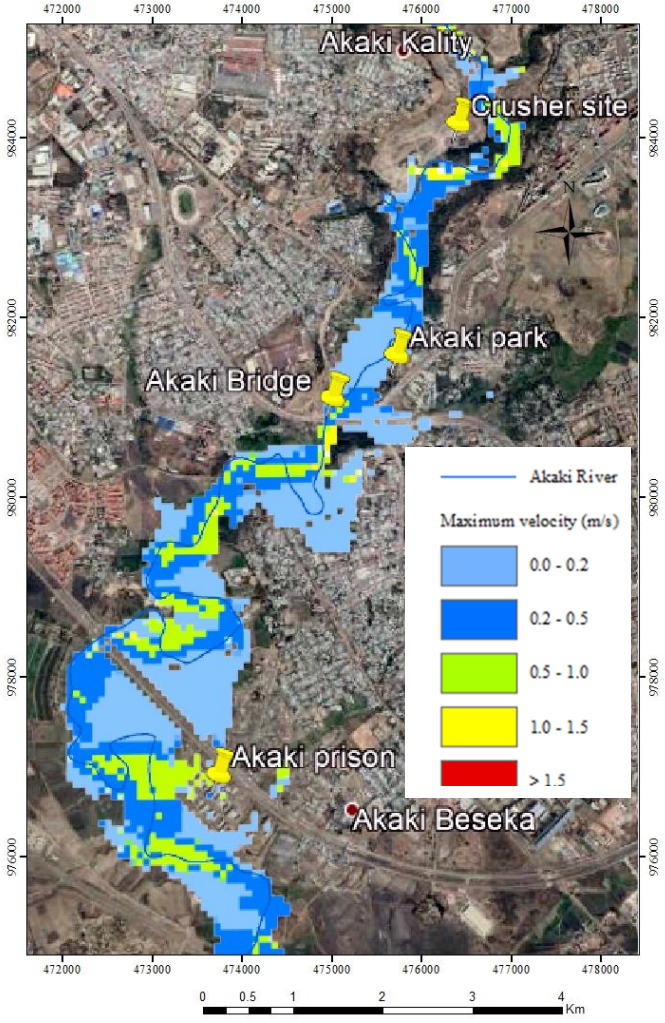

Figure 4-10 Maximum flood velocity maps for the simulation using two tributaries and cross-section from corrected DEM

5 CONCLUSION AND RECOMMENDATION

5.1 Conclusion

In this study, flood inundation mapping was conducted for different conditions depending on the change of DEM and tributary information. As a result, four (4) models were developed for each condition (for uncorrected DEM, for corrected DEM, by considering one tributary in the corrected DEM, and by considering two tributaries in the corrected DEM). The corrected DEM was developed by integrating the original or raw 5 m resolution DEM with 15 field-collected cross-section data. In the other case, two major tributary Rivers were identified and evaluated their contribution in flood simulation. Water level data was collected during a flood event in the rainy season of 2020 to serve as reference to evaluate effects of model inputs on the simulated water level.

The DEM captures the overall pattern of the observed channel cross-section profile but has limitation in capturing the actual channel width and depth. It was identified that the mismatch between the uncorrected and field cross-sections is caused by the resolution of the DEM, and the difference in data collection time of the raw DEM and field cross-section data. The applied DEM correction was successful in modifying the DEM cross-section to have similar characteristics as the field-collected cross-section.

The use of various downstream boundary condition caused significant difference in the simulated water level up to a distance of 3.5km upstream of the downstream boundary site. This indicates the importance of appropriately fixing the location and type of downstream boundary condition for flood modelling in the Akaki floodplain.

Flood water level simulations were found to have large mean absolute error (1.65m) when the uncorrected DEM was used and the contribution of the tributaries is not considered. This significantly reduced to 0.84m when the DEM was corrected using field measured cross-section data and dropped to 0.36m when the contribution of one tributary is considered. However, considering the second tributary slightly deteriorated the accuracy in terms of mean absolute error. Even though reduction is model error was attained when correcting the channel cross-section from the DEM and improving representation of the upstream boundary condition, the error is still large indicating the contribution of other factors on the accuracy of flood modeling in the study area cannot be ignored.

Modeling using the uncorrected DEM and ignoring the contribution of the two tributaries (i.e. the input data error) resulted in up to 0.21 km^2 difference in the simulated flood extent. This also resulted in large differences in flood depth and velocity over the study area. Besides, the resulted flood depth was small (8.03m) when the uncorrected DEM was used and it turns into maximum (9.42m) when the contribution of one tributary is considered. Overall, a difference of the input data source results in up to 1.22m difference in the simulated flood depth. In addition, the resulted flood velocity was small (9.49m/s) when the uncorrected DEM was used and the contribution of the tributaries is not considered. This significantly increases to 24.06m/s when the contribution of the second tributary is considered. Overall, a difference of the input data source results in up to 14.57 m/s difference in the simulated flood velocity.

5.2 Recommendation

Similar too many floodplains, there is critical data gap in the Akaki floodplain to properly set-up, calibrate and validate hydrodynamic flood models. In this study, it was demonstrated that the water level data that is collected in collaboration with a local resident was very valuable for flood modelling. However, most flood events resulted in peaks during nighttime which restricted manual measurement of water level. Therefore, installing automatic water level sensor can help to fill this gap while still engaging the local residents in data collection. It was demonstrated here that cross-section data can be collected without using expensive surveying equipment. However, this was time consuming and some areas were inaccessible. Hence, use of drones (e.g. equipped with LIDAR sensors) for mapping the channel topography can be investigated in the future.

Today uncertainty analysis is an inseparable part of the model prediction. As a result, further study needs to identify, quantify, and rank different sources of uncertainty and their impacts on flood simulation. In this study, further study is needed to map flood inundation by incorporating water level data that is measured in the tributary. In addition, incorporating effect of other input data's are required.

This study is concerned flood inundation mapping using 1D. Further, it is recommended to consider 2D or coupling 1D and 2D HEC RAS model. In addition flood inundation should be prepared for different return periods. Finally, it is recommended to collect spatially distributed flood depth and extent data using citizen scientists' observation for calibration and evaluation of the flood model.

REFERENCE

Abbas, S. A., Al-aboodi, A. H., & Ibrahim, H. T. (2020). Identification of Manning's Coefficient Using HEC-RAS Model : Upstream Al-Amarah Barrage. 2020.

Abily, M., Bertrand, N., Delestre, O., Gourbesville, P., & Duluc, C. (2016). Environmental Modelling & Software Spatial Global Sensitivity Analysis of High Resolution classi fi ed topographic data use in 2D urban fl ood modelling. Environmental Modelling and Software, 77, 183–195. https://doi.org/10.1016/j.envsoft.2015.12.002

Abo-El-Wafa, H., Yeshitela, K., & Pauleit, S. (2018). The use of urban spatial scenario design model as a strategic planning tool for Addis Ababa. Landscape and Urban Planning, 180(August 2015), 308–318. https://doi.org/10.1016/j.landurbplan.2017.08.004

Achamyeleh, K. (2003). Integrated flood management. 1–5 https://www.floodmanagement.info/publications/casestudies/cs_ethiopia_syn.pdf.

Afshari, S., Tavakoly, A. A., Adnan, M., Zheng, X., Follum, M. L., Omranian, E., & Fekete, B. M. (2018). Comparison of new generation low-complexity flood inundation mapping tools with a hydrodynamic model. Journal of Hydrology, 556, 539–556. https://doi.org/10.1016/j.jhydrol.2017.11.036

Ali, M. (2016).Flood Inundation Modeling and Hazard Mapping under Uncertainty in the Sungai Johor Basin , Malaysia.

Arrighi, C. (2019). Effects of digital terrain model uncertainties on high-resolution urban flood damage assessment. December 2018, 1–12. https://doi.org/10.1111/jfr3.12530

Bellos, V., Kourtis, I. M., Moreno-rodenas, A., & Tsihrintzis, V. A. (n.d.). Quantifying Roughness Coefficient Uncertainty in Urban Flooding Simulations through a Simplified Methodology. https://doi.org/10.3390/w9120944

Bertrand, N., Abily, M., Delestre, O., Amoss, L., Duluc, C., Gourbesville, P., & Navaro, P. (2015). Uncertainty related to high resolution topographic data use for flood event modeling over urban areas : toward a sensitivity analysis approach. 48(january), 385–399.

Bessar, M. A., Matte, P., & Anctil, F. (2020). Uncertainty analysis of a 1D river hydraulic model with adaptive calibration. Water (Switzerland), 12(2). https://doi.org/10.3390/w12020561

Bhagabati, S. S., Kawasaki, A., Takeuchi, W., & Zin, W. W. (2020). Improving river bathymetry and topography representation of a low-lying flat River Basin by integrating multiple sourced datasets. Journal of Disaster Research, 15(3), 335–343. https://doi.org/10.20965/jdr.2020.p0335

Bhola, P. K., Leandro, J., & Disse, M. (2019). Reducing uncertainties in flood inundation outputs of a two-dimensional hydrodynamic model by constraining roughness. 1445–1457.

Birhanu, D., Kim, H., Jang, C., & Park, S. (2016). Flood Risk and Vulnerability of Addis Ababa City Due to Climate Change and Urbanization. Procedia Engineering, 154, 696–702. https://doi.org/10.1016/j.proeng.2016.07.571

Borner, K., Boyack, K., Strategies, S., & Milojevic, S. (2012). Models of Science Dynamics. May 2014. https://doi.org/10.1007/978-3-642-23068-4

Brunner, G. W., & CEIWR-HEC. (2016). HEC-RAS River Analysis System User's Manual. US Army Corps of Engineers–Hydrologic Engineering Center. January, 1–790. https://www.hec.usace.army.mil/software/hec-ras/documentation/HEC-RAS 5.0 Users Manual.pdf

Chow, V. (1959). Applied Hydrology.

CLUVA. (2012). Climate change and vulnerability of African cities. Research briefs for Dar es Salaam,Tanzania. June, 1–29.

Conway, D., Mould, C., & Bewket, W. (2004). Over one century of rainfall and temperature observations in Addis Ababa, Ethiopia. International Journal of Climatology, 24(1), 77–91. https://doi.org/10.1002/joc.989

Costabile, P., Costanzo, C., Ferraro, D., Macchione, F., & Petaccia, G. (2020). Performances of the new HEC-RAS version 5 for 2-D hydrodynamic-based rainfall-runoff simulations at basin scale: Comparison with a state-of-the art model. Water (Switzerland), 12(9), 1–19. https://doi.org/10.3390/W12092326

Cukrov, G. (2013). Using Stereo Photogrammetry to Create Digital Elevation Models of Planetary Surfaces. 2013 Ncur, 0(0), 1–4. http://www.ncurproceedings.org/ojs/index.php/NCUR2013/article/view/585

Demlie, M., Wohnlich, S., Wisotzky, F., & Gizaw, B. (2007). Groundwater recharge, flow and hydrogeochemical evolution in a complex volcanic aquifer system, central Ethiopia. Hydrogeology Journal, 15(6), 1169–1181.

Denn, K. (2014). T wo-dimensional capabilities of hec-ras.

Devia, G. K., Ganasri, B. P., & Dwarakish, G. S. (2015). A Review on Hydrological Models. Aquatic Procedia, 4(July), 1001–1007. https://doi.org/10.1016/j.aqpro.2015.02.126

Dimitriadis, P., Tegos, A., Oikonomou, A., Pagana, V., Koukouvinos, A., Mamassis, N., Koutsoyiannis, D., & Efstratiadis, A. (2016). Comparative evaluation of 1D and quasi-2D hydraulic models based on benchmark and real-world applications for uncertainty assessment in flood mapping. Journal of Hydrology, 534, 478–492. https://doi.org/10.1016/j.jhydrol.2016.01.020

Douglas, I., Alam, K., Maghenda, M., Mcdonnell, Y., Mclean, L., & Campbell, J. (2008). Unjust waters: Climate change, flooding and the urban poor in Africa. Environment and Urbanization, 20(1), 187–205. https://doi.org/10.1177/0956247808089156

Doyle, A., Hynes, W., & Purcell, S. M. (2020). Enhancing Urban Resilience. July, 282–304. https://doi.org/10.4018/978-1-7998-4018-3.ch011

Ersoy, M., Lakkis, O., & Townsend, P. (2020). A Saint-Venant Model for Overland Flows with Precipitation and Recharge. Mathematical and Computational Applications, 26(1), 1. https://doi.org/10.3390/mca26010001

Federal Democratic Republic of Ethiopia [FDRE]. (2018). Federal Democratic Republic of Ethiopia National Disaster Risk Management Commission, early Warning and Emergency Response Directorate Flood Alert (FDRMC) # 3. 3, 1–7.

Federal disaster prevantion and prepardeness agency. (2007). https://reliefweb.int/report/ethiopia/ethiopia-disaster-prevention-and-preparedness-agency-vol14-no1.

Feyissa, G., Zeleke, G., Gebremariam, E., & Bewket, W. (2018). GIS based quantification and mapping of climate change vulnerability hotspots in Addis Ababa. Geoenvironmental Disasters, 5(1). https://doi.org/10.1186/s40677-018-0106-4

Feyera, A. (2007). Modelling of Akaki river liquid waste disposal and base flow separation. July.

Fire & Emergency prevention and rescue agency. (2018). 15, 1–3. Flood vulnerable places in 2018 and Vulnerability label in Addis Ababa

Fujisada, H., Urai, M., & Iwasaki, A. (2020). Manual-based improvement method for the ASTER global water body data base. Remote Sensing, 12(20), 1–11. https://doi.org/10.3390/rs12203373

Gebre SL, G. Y. (2015). Flood Hazard Assessment and Mapping of Flood Inundation Area of the Awash River Basin in Ethiopia using GIS and HEC-GeoRAS/HEC-RAS Model. Journal of Civil & Environmental Engineering, 05(04). https://doi.org/10.4172/2165-784x.1000179

Haile, T. Re. (2010). Uncertainty issues in hydrodynamic flood modeling Alemseged T. H. Building.

Hendrikse, J. H. (2003). Use of the Spatial Reference Object Model to enhance Projection and Datum Transformation. Geo-Information Science and Earth Observation, 376.

Arcement, Jr., George j and Verne r. Schneider (1989).Guide for Selecting Manning's Roughness Coefficients for Natural Channels and Flood Plains

Hummel, S., Hudak, A. T., Uebler, E. H., Falkowski, M. J., & Megown, K. A. (2011). A comparison of accuracy and cost of LiDAR versus stand exam data for landscape management on the Malheur National Forest. Journal of Forestry, 109(5), 267–273. https://doi.org/10.1093/jof/109.5.267

Hunter, N. M., Bates, P. D., Horritt, M. S., & Wilson, M. D. (2007). Simple spatially-distributed models for predicting flood inundation: A review. Geomorphology, 90(3–4), 208–225. https://doi.org/10.1016/j.geomorph.2006.10.021

Hutanu, E., Mihu-Pintilie, A., Urzica, A., Paveluc, L. E., Stoleriu, C. C., & Grozavu, A. (2020). Using 1D HEC-RAS modeling and LiDAR data to improve flood hazard maps accuracy: A case study from Jijia Floodplain (NE Romania). Water (Switzerland), 12(6), 1–21. https://doi.org/10.3390/w12061624

Jalayer, F., De Risi, R., De Paola, F., Giugni, M., Manfredi, G., Gasparini, P., Topa, M. E., Yonas, N., Yeshitela, K., Nebebe, A., Cavan, G., Lindley, S., Printz, A., & Renner, F.

(2014). Probabilistic GIS-based method for delineation of urban flooding risk hotspots. Natural Hazards, 73(2), 975–1001. https://doi.org/10.1007/s11069-014-1119-2

Lea, D., Yeonsu, K., & Hyunuk, A. (2019). Case study of HEC-RAS 1D-2D coupling simulation: 2002 Baeksan flood event in Korea. Water (Switzerland), 11(10). https://doi.org/10.3390/w11102048

Leupi, C., Souhar, O., Paquier, A., & Faure, J. (2016). Automatic Assessment of Uncertainties in the Case of Urban Flood Modeling. 2060(May). https://doi.org/10.1080/19942060.2009.11015283

Ethiopia Road Authority E. R. A. (2013). Drainage design manual (Source: ERA Website).

McGranahan, G., Balk, D., & Anderson, B. (2007). The rising tide: Assessing the risks of climate change and human settlements in low elevation coastal zones. Environment and Urbanization, 19(1), 17–37. https://doi.org/10.1177/0956247807076960

Md Ali, A., Solomatine, D. P., & Di Baldassarre, G. (2015). Assessing the impact of different sources of topographic data on 1-D hydraulic modelling of floods. Hydrology and Earth System Sciences, 19(1), 631–643. https://doi.org/10.5194/hess-19-631-2015

Medeiros, S. C., Hagen, S. C., & Weishampel, J. F. (2012). Comparison of floodplain surface roughness parameters derived from land cover data and field measurements. Journal of Hydrology, 452–453, 139–149. https://doi.org/10.1016/j.jhydrol.2012.05.043

Michele, F., Aawa, G. F., Gero, M., Willis, F. T., Paul, B., Unibristol, N. J., Giuliano, D. B., & Ihe, B. T. (2011). Critical review of non structural measures for water related risks. Kulturisk Project, 31(0), 1–42.

Nkwunonwo, U. C., Whitworth, M., & Baily, B. (2020). A review of the current status of flood modelling for urban flood risk management in the developing countries. Scientific African, 7(March), e00269. https://doi.org/10.1016/j.sciaf.2020.e00269

National Mertological Agency (2006). Climate change national adaptation program of action (NAPA) of Ethiopia

Office for the Coordination of Humanitarian Affairs (OCHA) . , (2020) . Ethiopia : Floods. https://reliefweb.int/report/ethiopia/ethiopia-floods-flash-update-5-may-2020.

Ozdemir, H., Sampson, C. C., De Almeida, G. A. M., & Bates, P. D. (2013). Evaluating scale and roughness effects in urban flood modelling using terrestrial LIDAR data. Hydrology and Earth System Sciences, 17(10), 4015–4030. https://doi.org/10.5194/hess-17-4015-2013

Pappenberger, F., Matgen, P., Beven, K. J., Henry, J. B., Pfister, L., & Fraipont, P. (2006). Influence of uncertain boundary conditions and model structure on flood inundation predictions. Advances in Water Resources, 29(10), 1430–1449. https://doi.org/10.1016/j.advwatres.2005.11.012

Pappenberger, F., Medium, F., Weather, R., Karsten, S., & Vienna, L. S. (2007). Advances in Geosciences Sensitivity and uncertainty in flood inundation modelling – concept of an analysis framework. May 2014. https://doi.org/10.5194/adgeo-11-31-2007

Parhi, P. K. (2013). HEC-RAS Model for Mannnig ' s Roughness : A Case Study. 2013(July), 97–101.

Poretti, I., & De Amicis, M. (2011). An approach for flood hazard modelling and mapping in the medium Valtellina. Natural Hazards and Earth System Science, 11(4), 1141–1151. https://doi.org/10.5194/nhess-11-1141-2011

Pulighe, G., & Fava, F. (2013). DEM extraction from archive aerial photos: Accuracy assessment in areas of complex topography. European Journal of Remote Sensing, 46(1), 363–378. https://doi.org/10.5721/EuJRS20134621

Quiroga, V. M., Kure, S., Udo, K., & Mano, A. (2016). Application of 2D numerical simulation for the analysis of the February 2014 Bolivian Amazonia flood: Application of the new HEC-RAS version 5. RIBAGUA - Revista Iberoamericana Del Agu, 3(1), 25–33. https://doi.org/10.1016/j.riba.2015.12.001

Ramsbottom, D., & Wicks, J. (2003). Catchment Flood Management Plans: Guidance on Selection of Appropriate Hydraulic Modelling Methods. Environment Agency, Bristol, UK.

Sahoo, S. N., & Sreeja, P. (2017). Development of Flood Inundation Maps and Quantification of Flood Risk in an Urban Catchment of Brahmaputra River. ASCE-ASME Journal of Risk and Uncertainty in Engineering Systems, Part A: Civil Engineering, 3(1), 1–11. https://doi.org/10.1061/AJRUA6.0000822

Saksena, S., & Merwade, V. (2015). Incorporating the effect of DEM resolution and accuracy for

improved flood inundation mapping. Journal of Hydrology, 530, 180–194. https://doi.org/10.1016/j.jhydrol.2015.09.069

Sarhadi, A., Soltani, S., & Modarres, R. (2012). Probabilistic flood inundation mapping of ungauged rivers : Linking GIS techniques and frequency analysis. Journal of Hydrology, 458–459, 68–86. https://doi.org/10.1016/j.jhydrol.2012.06.039

Smith, M.J., Edwards, E.P., Priestnall, G., Bates, P. D. (2006). Exploitation of new data types to create digital surface models for flood inundation modeling. FRMRC Research Report UR3, FRMRC, UK. September. https://doi.org/10.13140/RG.2.2.29963.08487

Stephens, E. M., Bates, P. D., Freer, J. E., & Mason, D. C. (2012). The impact of uncertainty in satellite data on the assessment of flood inundation models. Journal of Hydrology, 414–415, 162–173. https://doi.org/10.1016/j.jhydrol.2011.10.040

Szypula, B. (2019). Quality assessment of DEM derived from topographic maps for geomorphometric purposes. Open Geosciences, 11(1), 843–865. https://doi.org/10.1515/geo-2019-0066

Tarekegn, T. H., Haile, A. T., Rientjes, T., Reggiani, P., & Alkema, D. (2010). Assessment of an ASTER-generated DEM for 2D hydrodynamic flood modeling. International Journal of Applied Earth Observation and Geoinformation, 12(6), 457–465. https://doi.org/10.1016/j.jag.2010.05.007

Teklie, N. (2017). Investigation on the Cause of High Way Flooding in Addis Ababa Addis Ababa February , 2017.

Teng, J., Jakeman, A. J., Vaze, J., Croke, B. F. W., Dutta, D., & Kim, S. (2017). Environmental Modelling & Software Flood inundation modelling : A review of methods , recent advances and uncertainty analysis. Environmental Modelling and Software, 90, 201–216. https://doi.org/10.1016/j.envsoft.2017.01.006

USACE. (2016). HEC-RAS River Analysis System Hydraulic Reference Manual Version 5.0. Hydrologic Engineering Center, February, 547.

Volunteers. (1995). Member of Japan overseas Cooperation. "Conditional survey and Fundamental Information on flood Affected Areas in Addis Ababa."

Vojtek, Andrea Petroselli, Jana Vojteková and Shahla Asgharinia. (2019). Flood inundation mapping in small and ungauged basins: sensitivity analysis using the EBA4SUB and HEC-RAS modeling approach Matej. 1002–1019. https://doi.org/10.2166/nh.2019.163

Ward, F. (2006). National meteorological agency agrometeorological bulletin. 16(9), 2–12.

Weatherill, N. (1998). Unstructured Grids. Handbook of Grid Generation, 136(August), 493–506. https://doi.org/10.1201/9781420050349.ch26

Werner, M. G. F. (2004). A comparison of flood extent modelling approaches through constraining uncertainties on gauge data. Hydrology and Earth System Sciences, 8(6), 1141–1152. https://doi.org/10.5194/hess-8-1141-2004

Willis, T., Wright, N., & Sleigh, A. (2019). Systematic analysis of uncertainty in 2D flood inundation models. Environmental Modelling and Software, 122(September), 104520. https://doi.org/10.1016/j.envsoft.2019.104520

Worako, A. W. (2016). Land Use Land Cover Change Detection by Using Remote Sensing Data in Akaki River Basin. October.

Yu, J. J., Qin, X. S., & Larsen, O. (2015). Uncertainty analysis of fl ood inundation modelling using GLUE with surrogate models in stochastic sampling. 1279(June 2014), 1267–1279. https://doi.org/10.1002/hyp.10249

Zeleňáková, M., Fijko, R., Labant, S., Weiss, E., Markovič, G., & Weiss, R. (2019). Flood risk modelling of the Slatvinec stream in Kružlov village, Slovakia. Journal of Cleaner Production, 212, 109–118. https://doi.org/10.1016/j.jclepro.2018.12.008

APPENDIX

Appendix A: Uncorrected, Field and Corrected River cross-section profile at different location

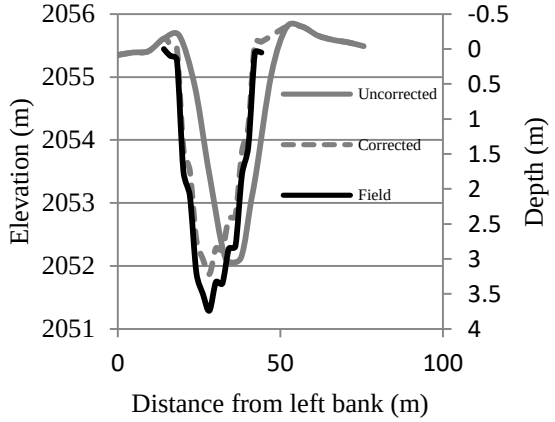

a. D/stream of the river around Kaliti village

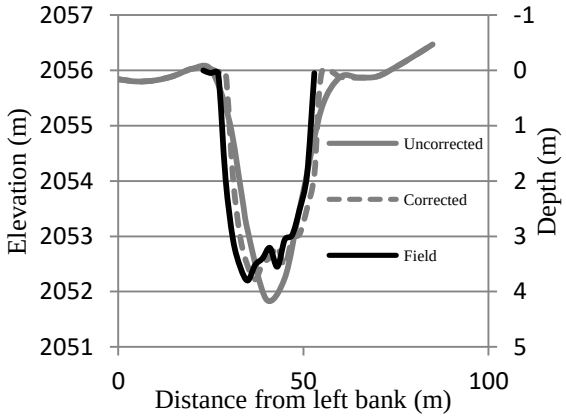

b. D/stream of the river around Condominium

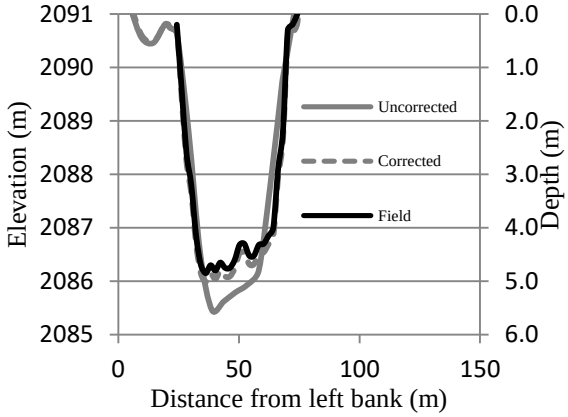

c. Upstream of the river around Crusher site

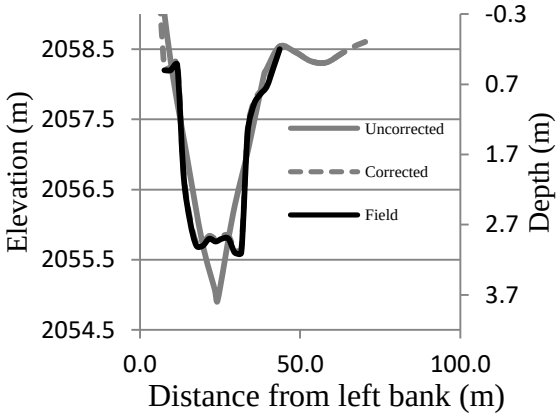

d. Middle of river Around Indian campus

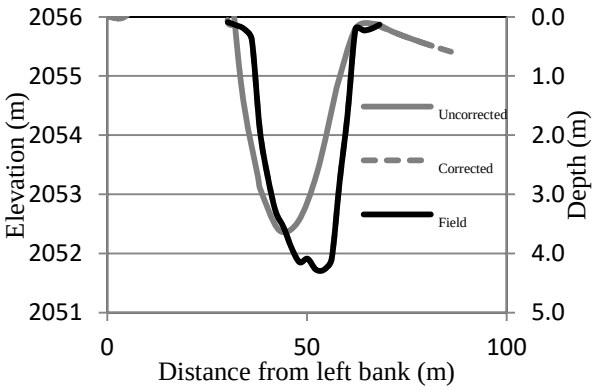

. e. D/stream of the river around grounding mill

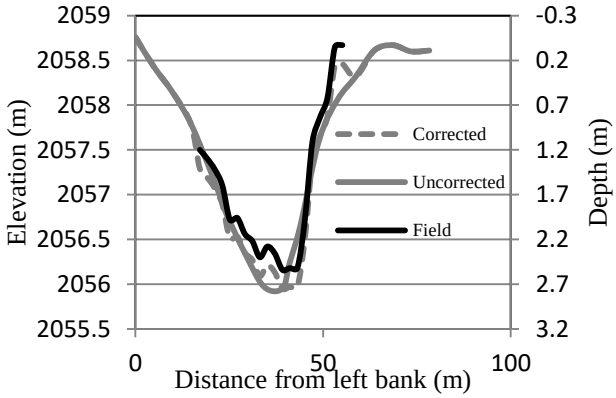

f. Middle of the river around wereda 8

Appendix B: Field water depths measured data at upstream (for simulating the model) and middle of the model domain (for evaluated simulated water levels) at different time.

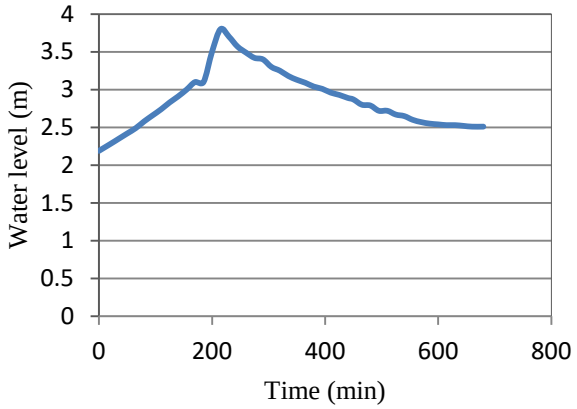

Upstream boundary condition (10/07/2020)

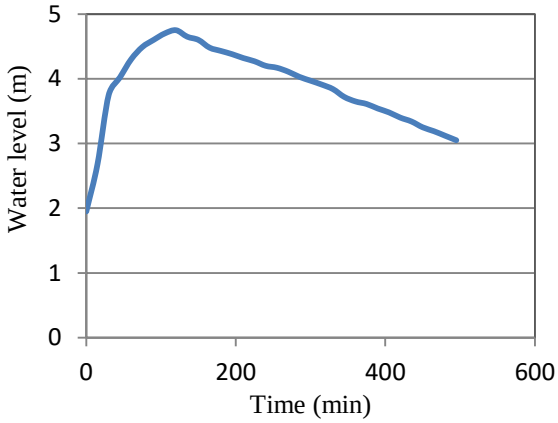

Validation data (10/07/2020)

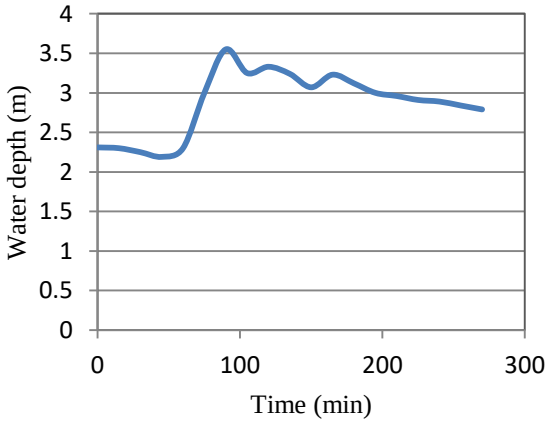

Upstream boundary condition (07/06/2020)

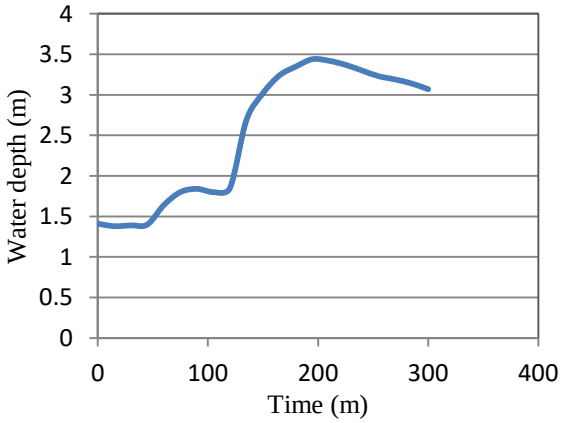

Validation data (07/06/2020)

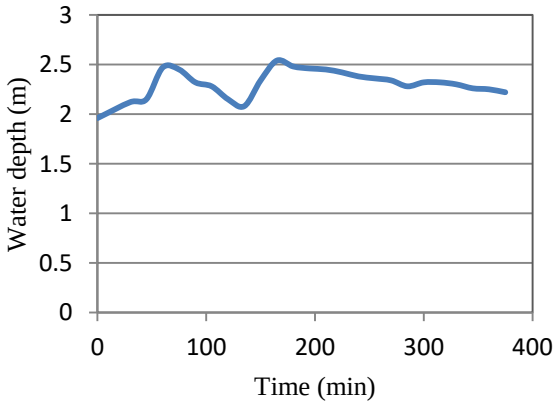

Upstream boundary condition (28/05/2020**)**

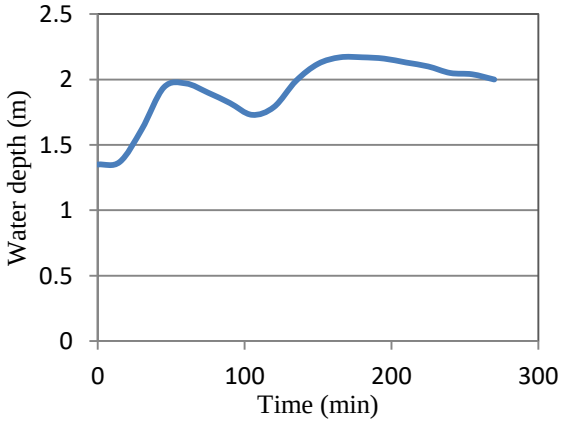

Validation data (28/05/2020)

Appendix C: Flood depth and velocity map result for the simulation using corrected & uncorrected DEM and consideration of one tributary

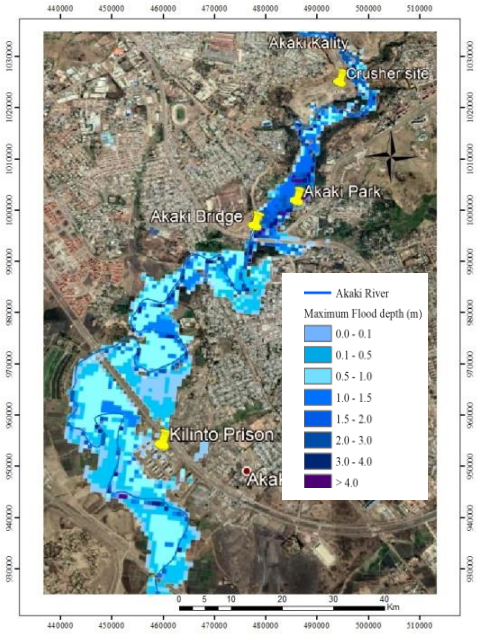

a.Flood depth for Uncorrected DEM

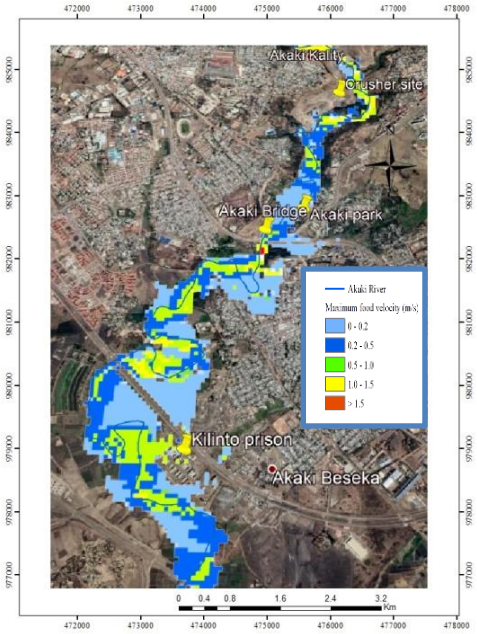

b. Flood velocity for uncorrected DEM

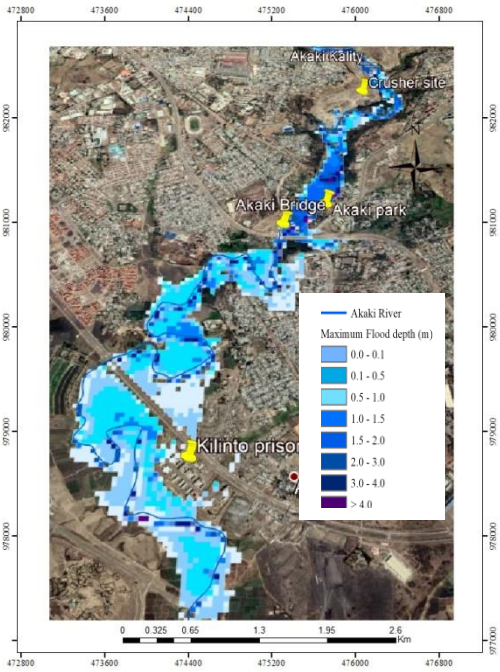

c. Flood depth for corrected DEM

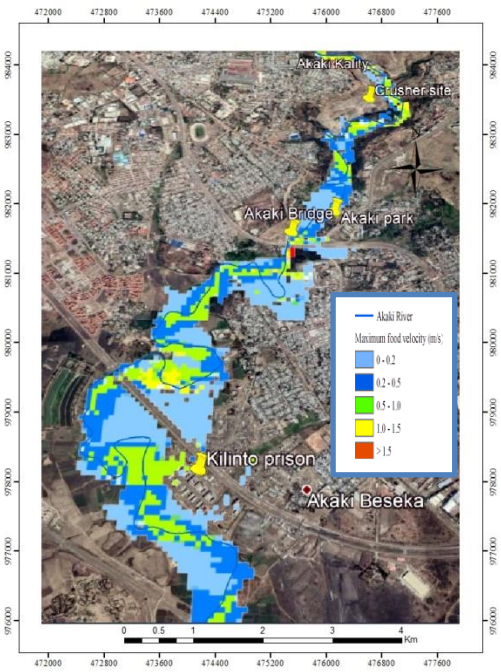

d. Flood velocity for corrected DEM

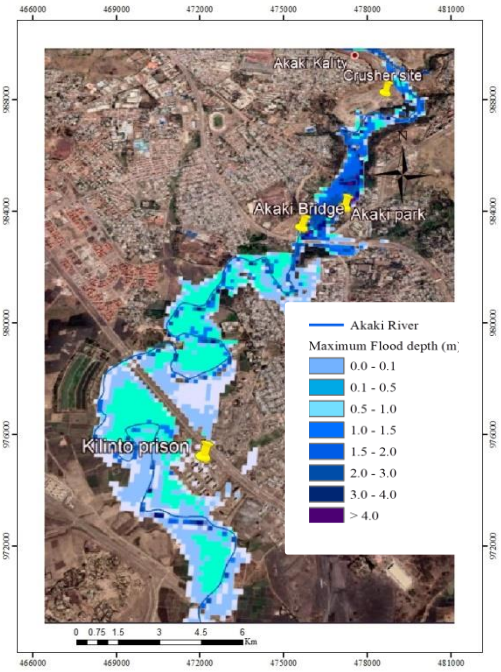

e. Flood depth for one tributary consideration

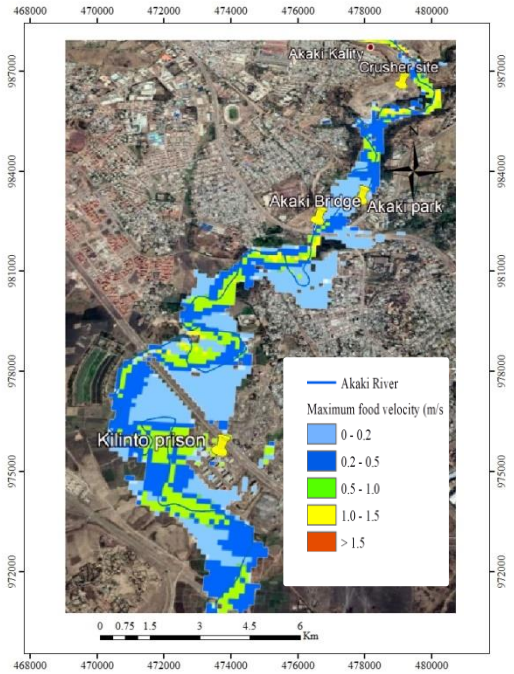

d. Flood velocity for one tributary consideration

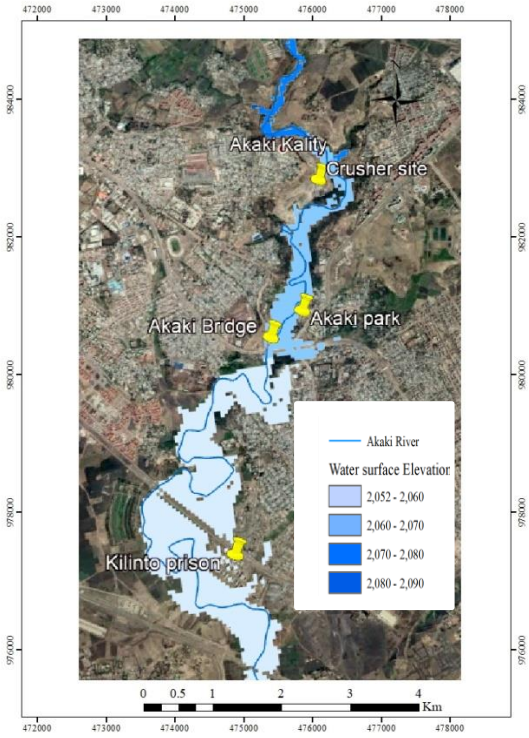

Figure: Maximum Water surface elevation for two tributary considerations

Appendix D: Sample photo that were collected during measuring flood data for Big Akaki River in the field.

a. Flood depth measurement around crusher site

b. flood inundation of 2020 summer season

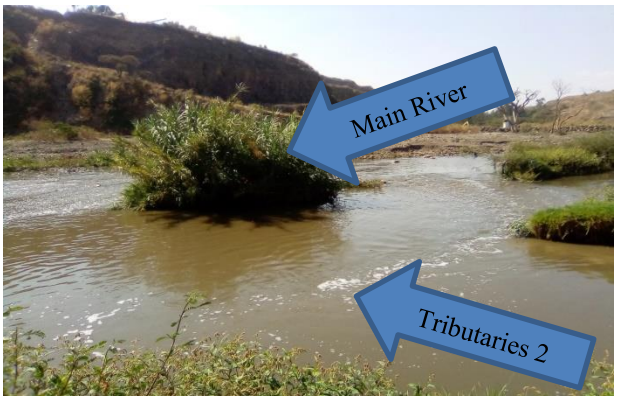

C. Joint of Main River and the first tributary

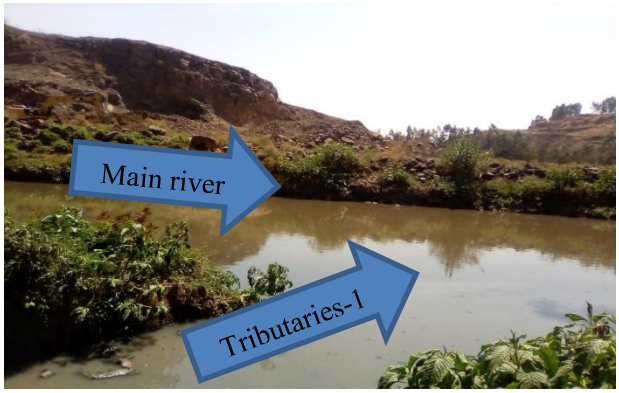

d. Joint of Main River and second tributary

e. Establishing the difference in elevation b/n the stakes

f. Flood overtopping during 2020 season

Appendix E: Flood Vulnerable places and Vulnerability label in Addis Ababa since 2018.

Table-1 Flood vulnerable places in 2018 in the sub-city of Addis Ababa (Fire & Emergency, 2018)

No.	Sub City	Vulnerable places (No.)			
		River over top	Poor Drainage pipe	Geographical location	Total
1	Arada	5	1	1	7
2	Kirkos	3	5		8
3	Addis Ketema	6	11		17
4	Lideta	2	3		5
5	Nifas Silk	8	7	3	18
6	Akaki	7	8	1	16
7	Bole	8	5	2	15
8	Yeka	7	2		9
9	Kolfe	13	20		33
10	Gulelle	8	4	3	15
Total		67	66	10	143

Table-2 Flood-prone area along major River and Vulnerability label in Addis Ababa source (Fire & Emergency, 2018)

River name	Flood prone area	Vulnerability label	Sub-city
Kebena river	Korea Veterans	High	Yeka
	Kidanemihiret cloister		Arada
	Germany Embassy		Yeka
	Selam Village around Bridge		Bole
	Congo village		Yeka
	Kebena square near the river		Yeka
	Oriel holly water		Bole

Kebena river	Yosefkese Village	High	Nifas Silk
	Chereka Village		Bole
	Hamele 19 Bridge		Yeka
Akaki river	Megala Village	Very High	Akaki Kaliti
	India campus		Akaki Kaliti
	Selam Health Center	High	Akaki Kaliti
	Sefare-Genet		Akaki Kaliti
	Abajele Village		Kolfe Keranio
	Germany Square	Medium	Nefas Silk
Little Akaki	Tura Bora	High	Akaki Kaliti
	Kayi Afer	Medium	Nifas Silk
Ginfille River	In front of women and Children's Hospital	High	Arada
	Back of Gibi-Gabriel		Arada
Ras Mekonine River	Ras Mekonine around Piasa	High	Arada
Bulebula river	Back of Bambis	High	Kirkos
Kidane-Mihiret River	-Back of Kidane-Mihiret Church	Medium	Gulelle
	Hamsa siminte	Medium	Nifas Silk
Bono Village River	District 05	High	Bole
	Egziabeherabe taxi		Bole
Shama Village River	District 5	High	Gulelle
Mariam River	Mariam River	High	Gulelle
Kara River	Back of Kera	Medium	Yeka
Efoyta River	District 02	High	Bole

Weji River	District 05	High	Bole
Shankila River	District 04	High	Addis Ketema
Musema River	Kuas Meda	High	Addis Ketema
Chaka River	Ahiya Berenda	High	Addis Ketema
Sheger Parking	Back of Sheger parking	High	Gulelle
Atorebi	Back youths Center	High	Gulelle
Esilam River	Back of Abebech Gobena Governorate	High	Arada
Welegemo tributaries river	Safere-Genet	High	Yeka
Yerer chora River	District 5	High	Bole
Dimdim River	Dimdim Wiha Bela Village	Very High	Akaki Kaliti
Lafto	Industry Parking	Low	Nifas silk
Yedili race River	Bihere Tsege	Medium	Nifas silk
Mamite abysm	Kesoch Village	High	Addis Ketema
River from Merkato	Chaka Village	High	Lideta
Burur River	Ayer tena(Mobil)	High	Kolfe Keranio
Anejeso River	Zenebe Werk(District 03)	High	Kolfe Keranio